



# Acceleration Relation in Dark Matter Problem from Dynamics to Lensing

Yong Tian 田 雍

Institute of Astronomy, National Central University

1st May, HEP Seminar, CYCU, Taoyuan

# Outline

## ➤ “Missing Mass Problem”

- History
- Flat Rotational Curve
- Tully-Fisher Relation
- Deficient Dark Matter in Elliptical Galaxies

## ➤ Acceleration Relation

- Spiral Galaxies
- Elliptical Galaxies

## ➤ Possibility - $\Lambda$ CDM & Modified Gravity

## ➤ Summary

# Dark Matter History

- In 1932, by studying stellar motions in the local galactic neighborhood, Oort found that the dynamical mass in the galactic plane must be greater than luminous mass.

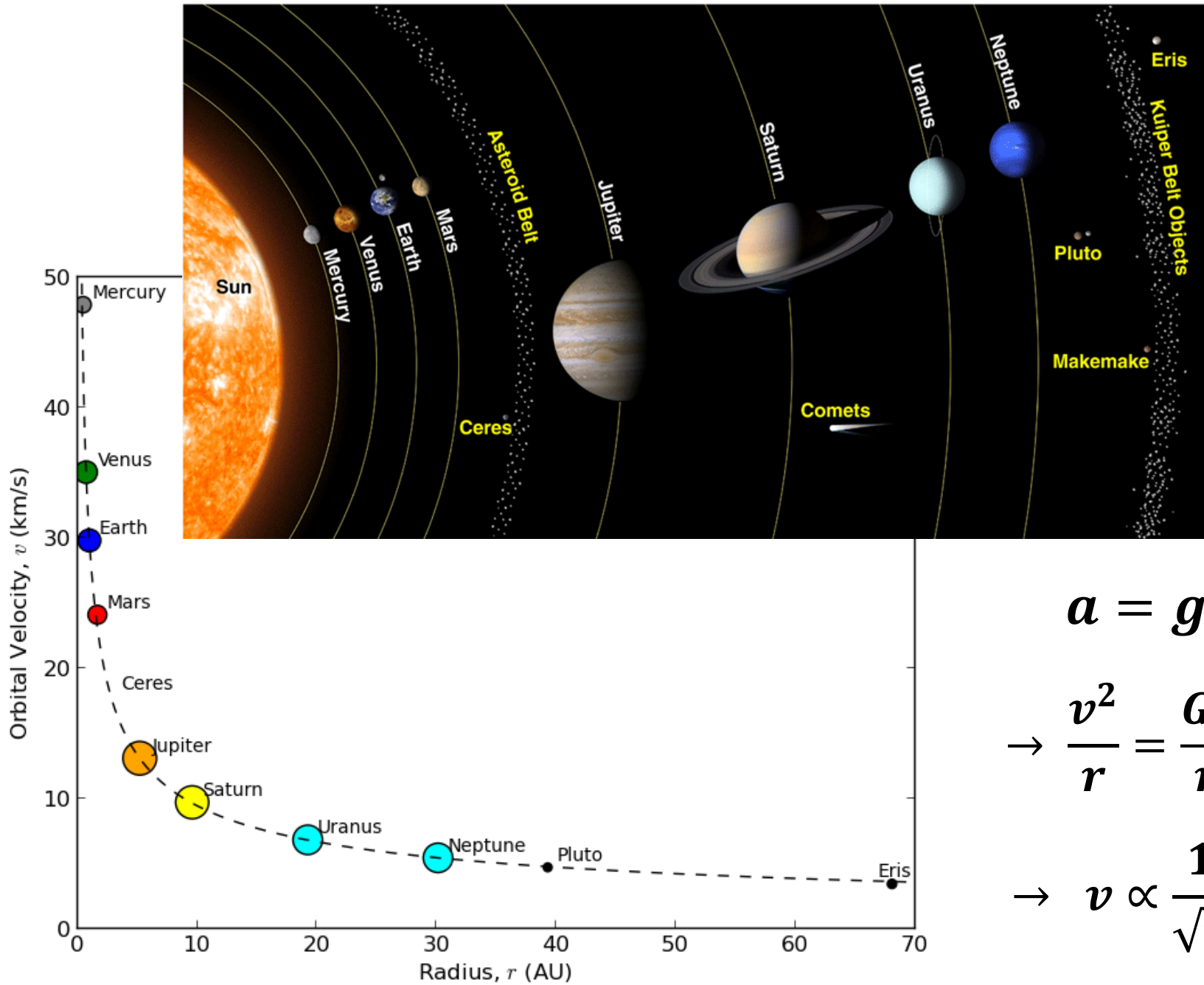


Jan Oort



Fritz Zwicky

- In 1933, Zwicky pointed out in Coma cluster the gravitational mass is larger than the luminous mass.
- Zwicky claims the existence of “Dark Matter” in Coma cluster.

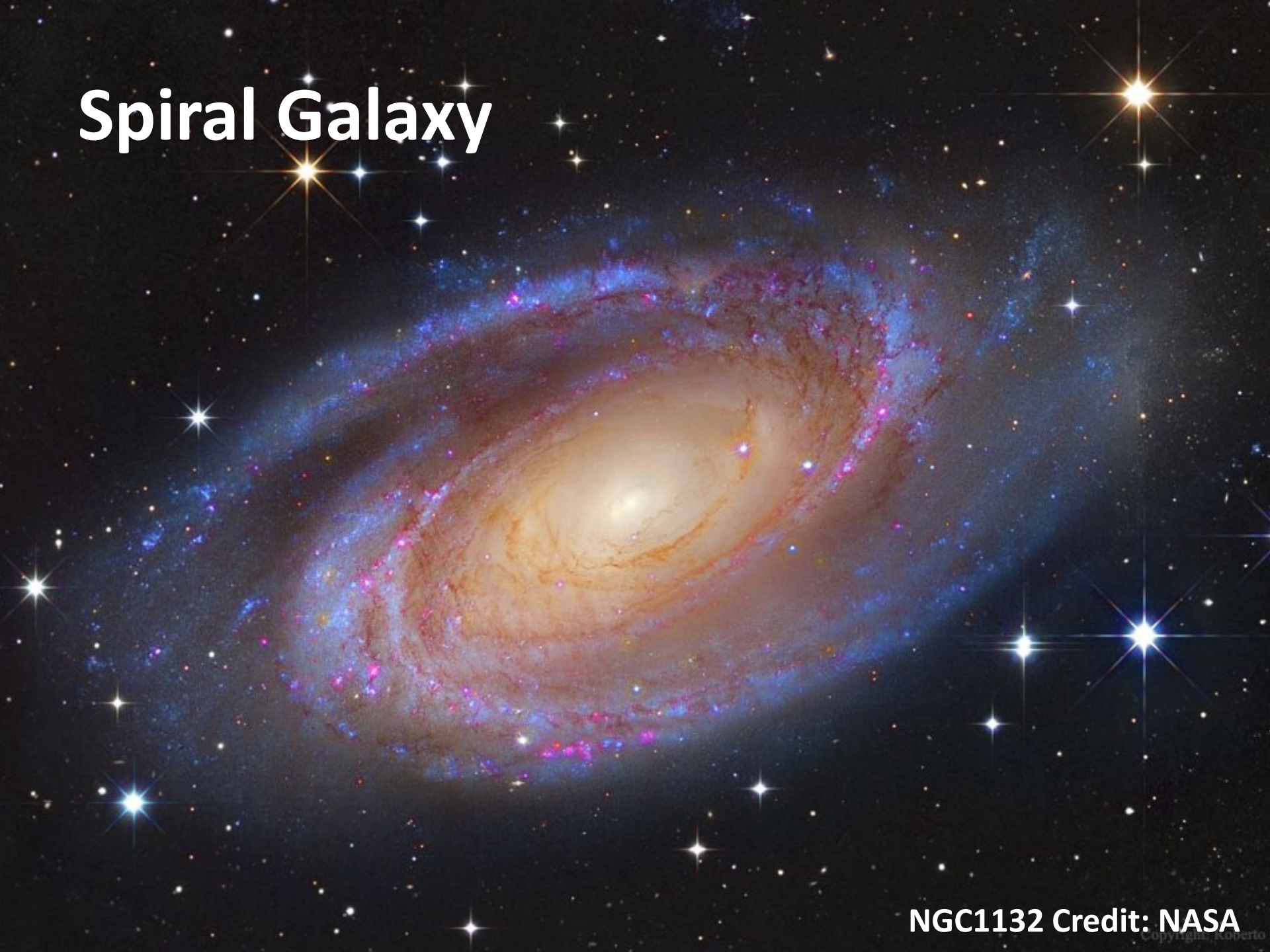


$$a = g$$

$$\rightarrow \frac{v^2}{r} = \frac{GM}{r^2}$$

$$\rightarrow v \propto \frac{1}{\sqrt{r}}$$

# Spiral Galaxy



NGC1132 Credit: NASA

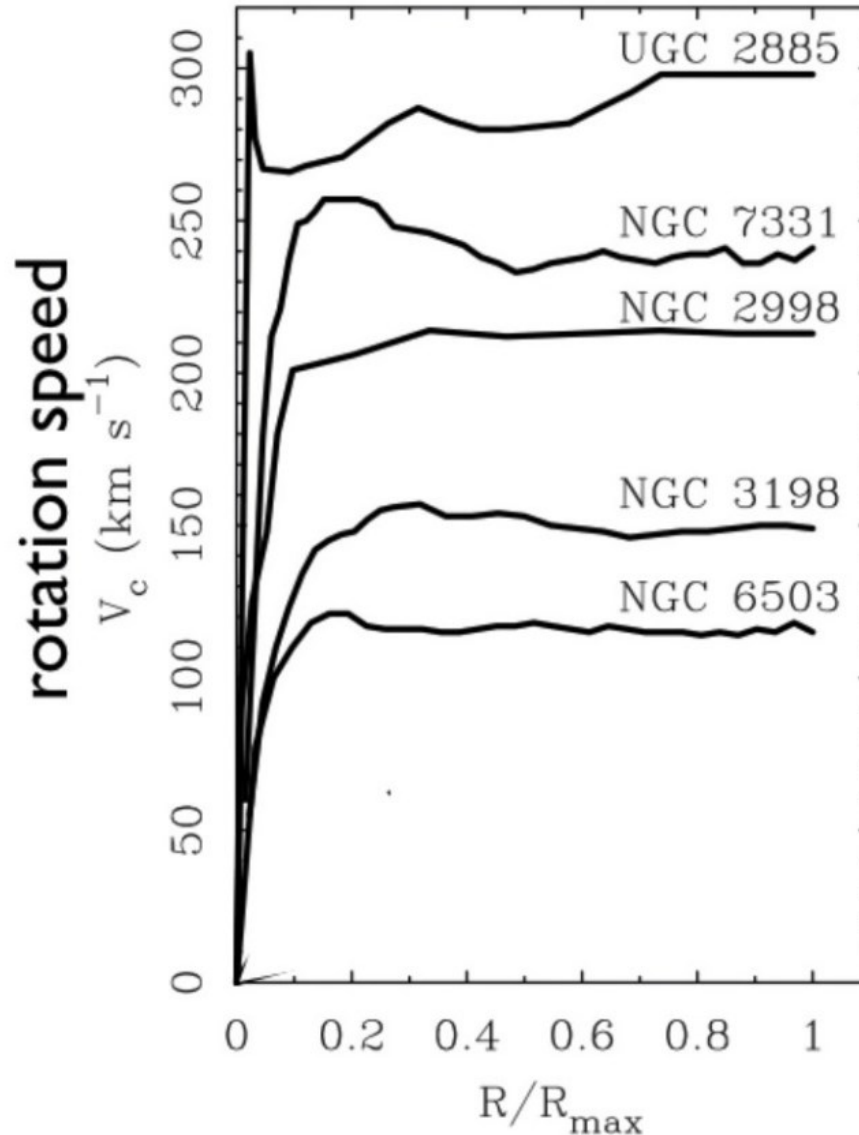


# Flat Rational Curves

Vera Rubin



Albert Bosma

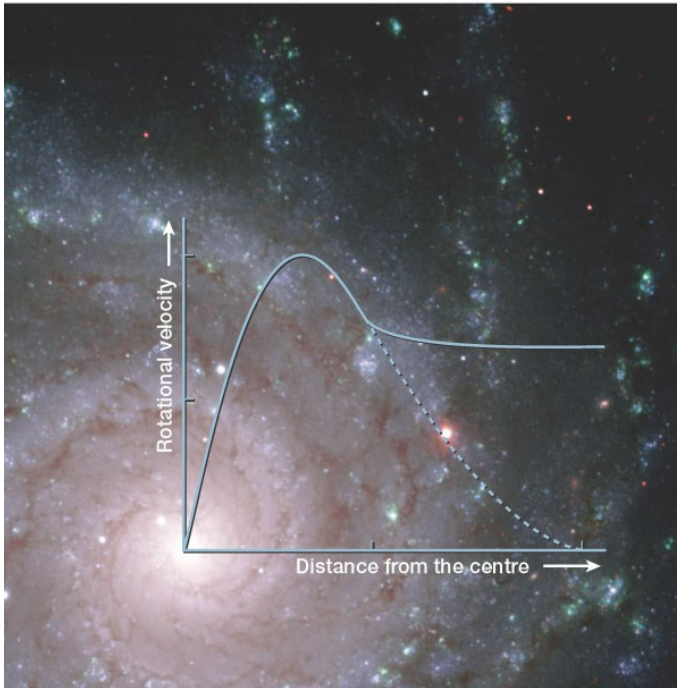


$$a = g$$

$$\rightarrow \frac{v^2}{r} = \frac{GM}{r^2}$$

$$\rightarrow v \propto \frac{1}{\sqrt{r}}$$

# The Tully-Fisher Relation



Fukugita, M., 2003, *Nature*, 422, 489

$$v^4 \propto L$$

$$\frac{v^2}{r} = \frac{GM}{r^2} \quad ?$$

R.B. Tully & M.J. Pierce, *ApJ*, 533, 744 (2000)

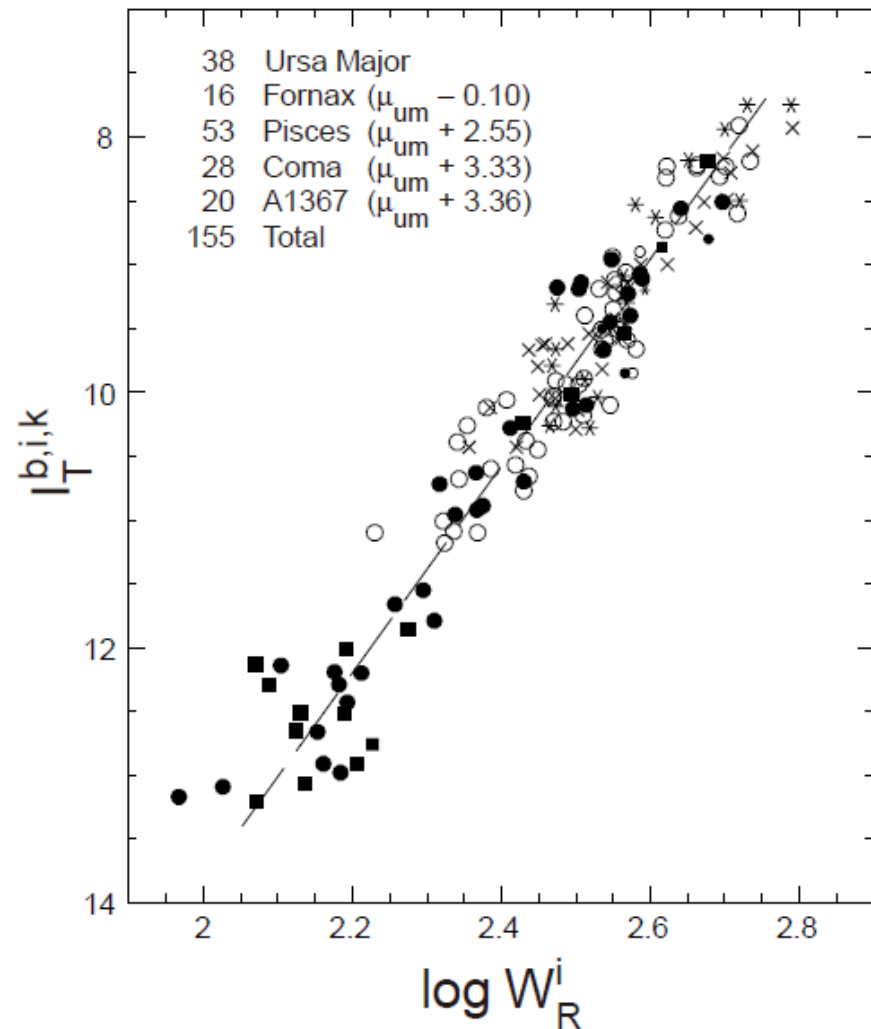


Figure 1.2: **Tully-Fisher Relation.** Total apparent magnitude in I band versus maximum rotational speed  $V_{max}$  in spiral galaxies, where  $V_{max} \sim \frac{1}{2}W_R^i$ . Left upper corner listed total 155 spiral galaxies in 5 clusters. Straight line represents a least squares fit to the ensemble. This diagram was first discovered by Tully & Fisher (1977). Here, it was refined by Tully & Pierce (2000).

# Elliptical Galaxy



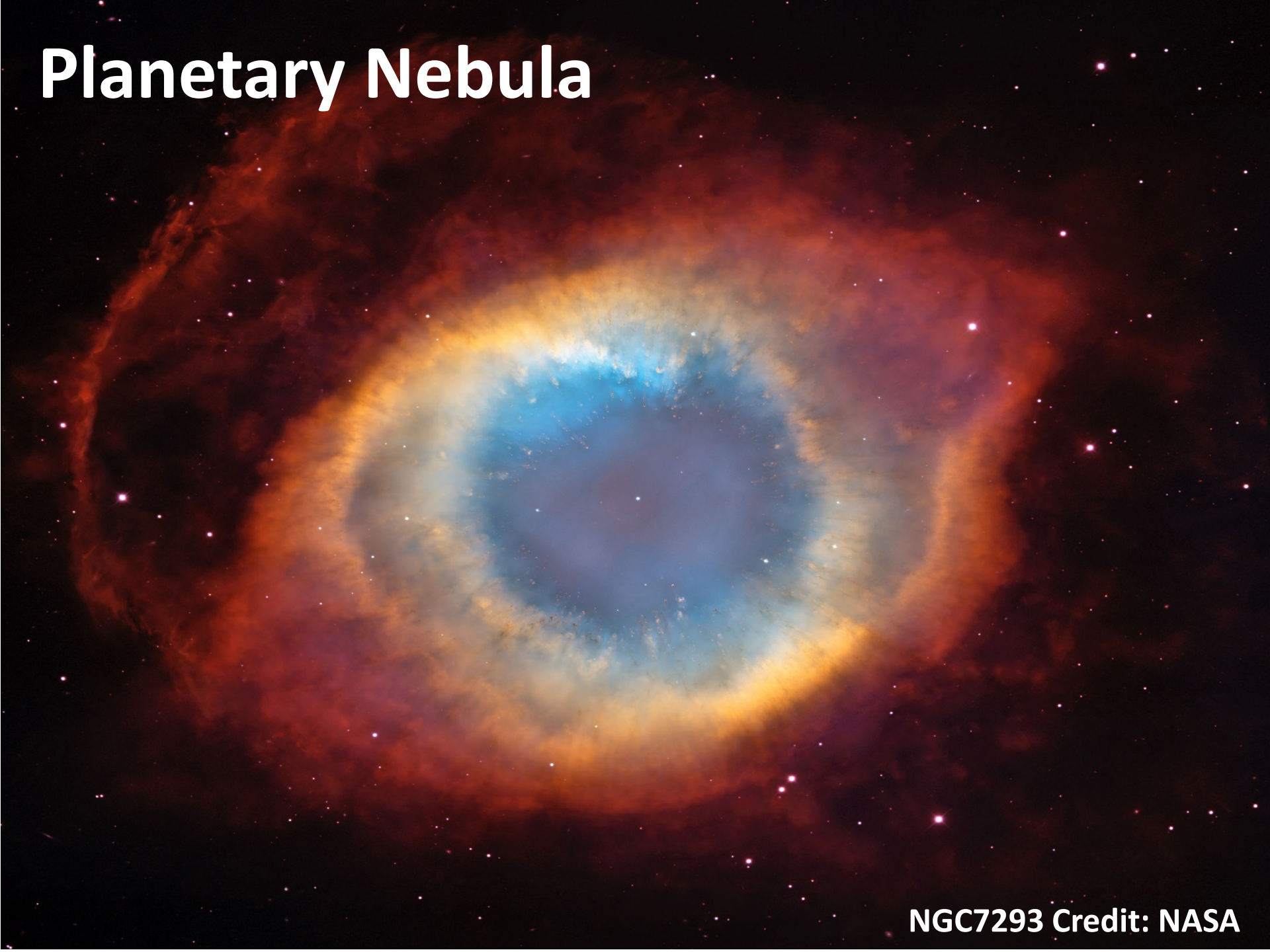
NGC1132 Credit: NASA



# Observation in Elliptical Galaxies

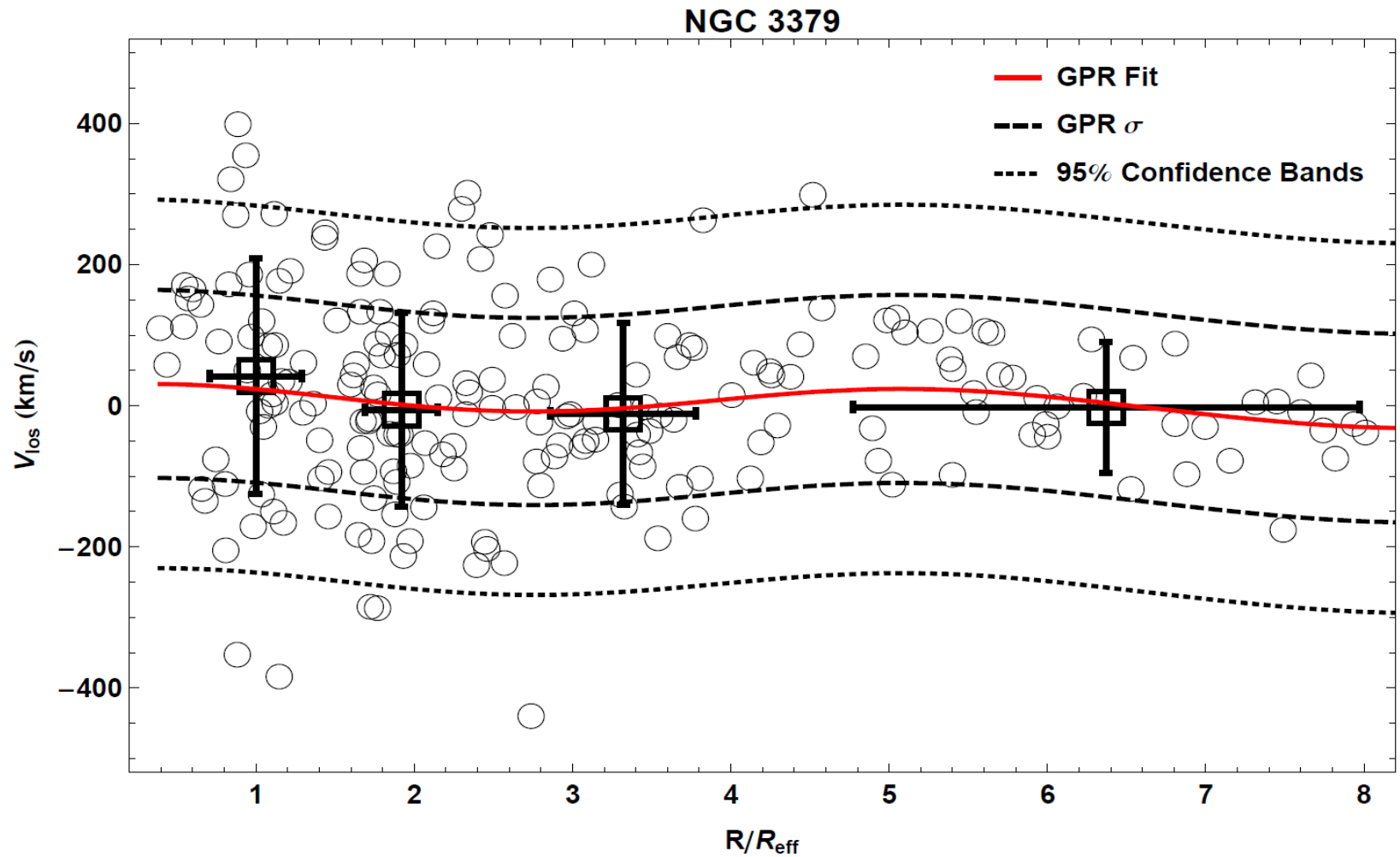
- As the surface brightness from the stars of elliptical galaxies drops rapidly beyond two effective radius (half-light radius), the kinematics of the galaxy at larger distances has to be studied by other sources.
- Motion of gas can be used in spiral galaxies but this is not suitable for elliptical galaxies as their gas content is low.
- Planetary Nebulae (PNe) and globular clusters have been suggested for elliptical galaxies.
- PNe are good tracers for velocity distribution because of their strong emission line O[III] at 500.7 nm.

# Planetary Nebula



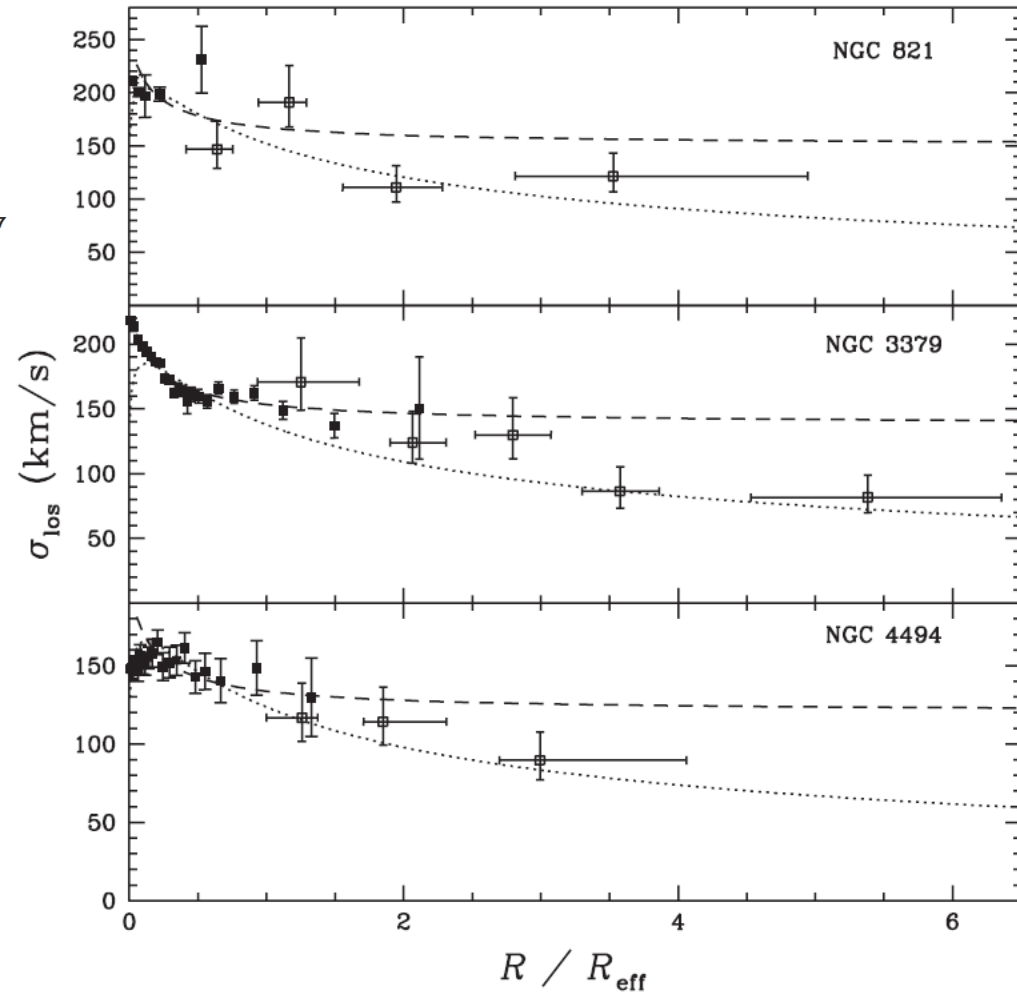
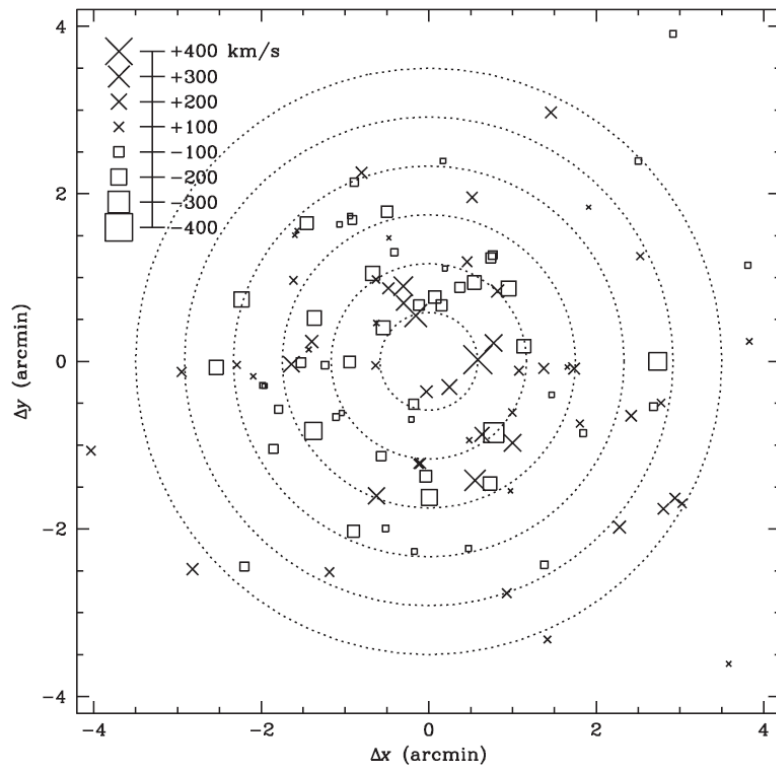
NGC7293 Credit: NASA

# Velocity Profile of PNe



## A Dearth of Dark Matter in Ordinary Elliptical Galaxies

Aaron J. Romanowsky,<sup>1,2\*</sup> Nigel G. Douglas,<sup>2</sup>  
 Magda Arnaboldi,<sup>3,4</sup> Konrad Kuijken,<sup>5,2</sup> Michael R. Merrifield,<sup>1</sup>  
 Nicola R. Napolitano,<sup>2</sup> Massimo Capaccioli,<sup>3,6</sup> Kenneth C. Freeman<sup>7</sup>



Galaxy	Type	$D$ (Mpc)	$R_{\text{eff}}$	$M_B$	Observations	$N(\text{PNs})$	$Y_{\text{BS}}(Y_{\text{B,C}})$
NGC 821	E2	24	50''	-20.5	Sep 2001, 11 hours	104	13-17
NGC 3379	E1	11	35''	-20.0	Mar 2002, 3 hours	109	5-8
NGC 4494	E0	17	49''	-20.6	Mar 2002, 4 hours	73	5-7

**Figure 1.3: NGC 3379 with 109 Planetary Nebula.** Crosses and boxes represent receding and approaching line of sight velocities respectively. The sizes of them listed on left upper corner are proportional to the velocity magnitudes. Dotted concentric circles are the radius with increment of effective radius  $R_{\text{eff}}$ . (Romanowsky (2003))



# MDAR

Mass Discrepancy-  
Acceleration Relation

## THE MASS DISCREPANCY–ACCELERATION RELATION: DISK MASS AND THE DARK MATTER DISTRIBUTION

STACY S. McGAUGH

Department of Astronomy, University of Maryland, College Park, MD 20742-2421; ssm@astro.umd.edu

*Received 2003 July 12; accepted 2004 March 25*

- **Observational acceleration** can be determined by rotational curve of spiral galaxy.

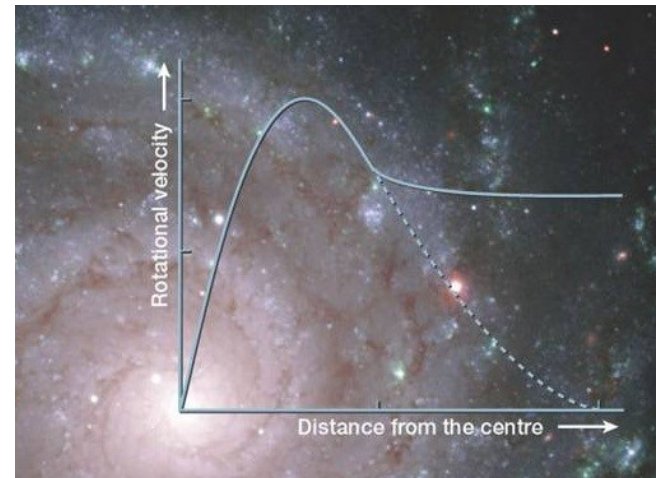
$$g_o(r) = \frac{V^2}{r} \qquad g_o(r) = \frac{GM_o(< r)}{r^2}$$

- **Baryonic acceleration** can be estimated by stellar and gas.

$$g_B(r) = \frac{GM_B(< r)}{r^2}$$

- **Mass discrepancy** can be decided by acceleration ratio.

$$g(r) = \frac{GM(< r)}{r^2} \rightarrow \frac{M_o(< r)}{M_B(< r)} = \frac{g_o(r)}{g_B(r)}$$

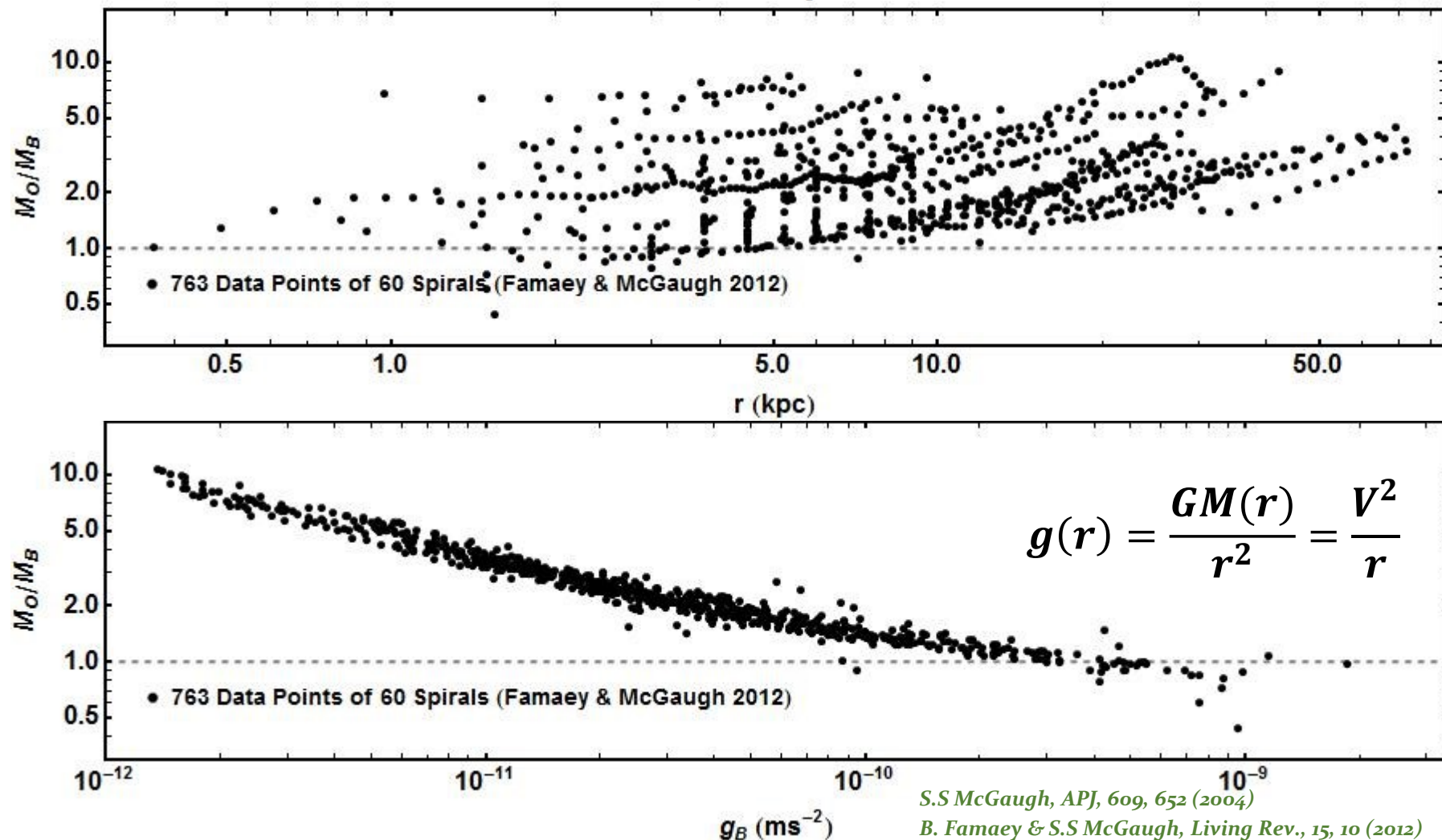


# THE MASS DISCREPANCY–ACCELERATION RELATION: DISK MASS AND THE DARK MATTER DISTRIBUTION

STACY S. MCGAUGH

Department of Astronomy, University of Maryland, College Park, MD 20742-2421; ssm@astro.umd.edu

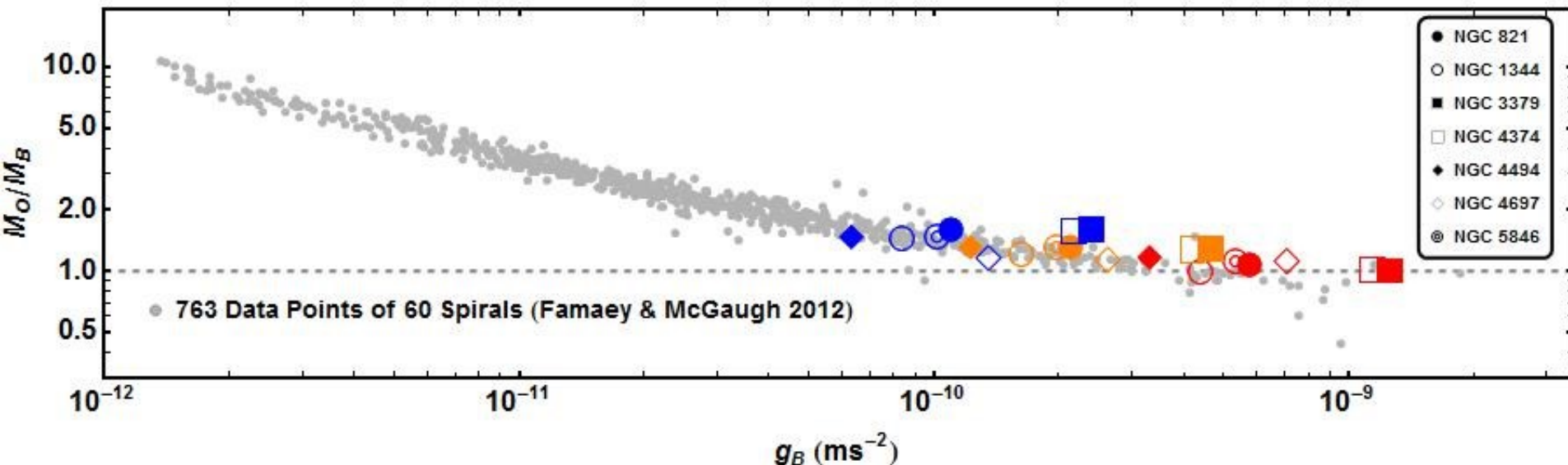
*Received 2003 July 12; accepted 2004 March 25*



# Dynamics of elliptical galaxies with planetary nebulae in modified Newtonian dynamics

Yong Tian<sup>1</sup>★ and Chung-Ming Ko<sup>1,2</sup>★

The **Mass Discrepancy-Acceleration Relation (MDAR)** in elliptical galaxies with PNe at 1-3 effective radius ( $R_{\text{eff}}$ ).





# Acceleration Scale?

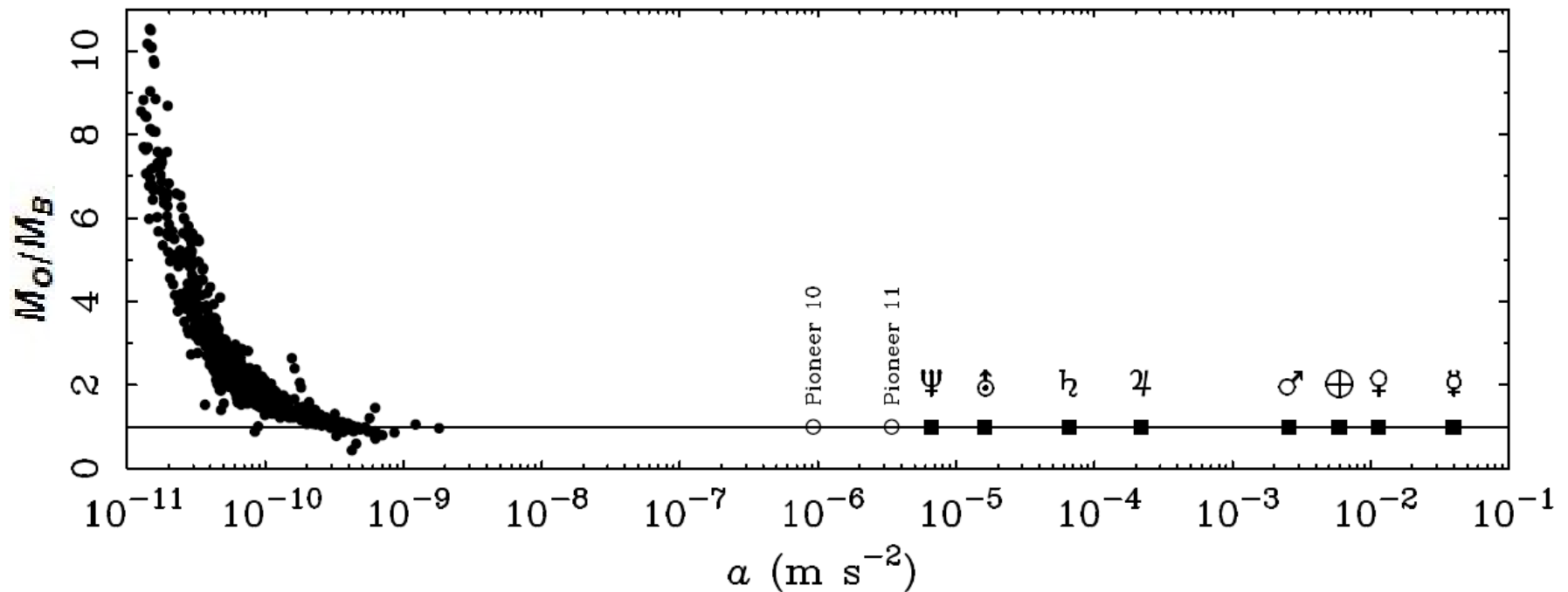
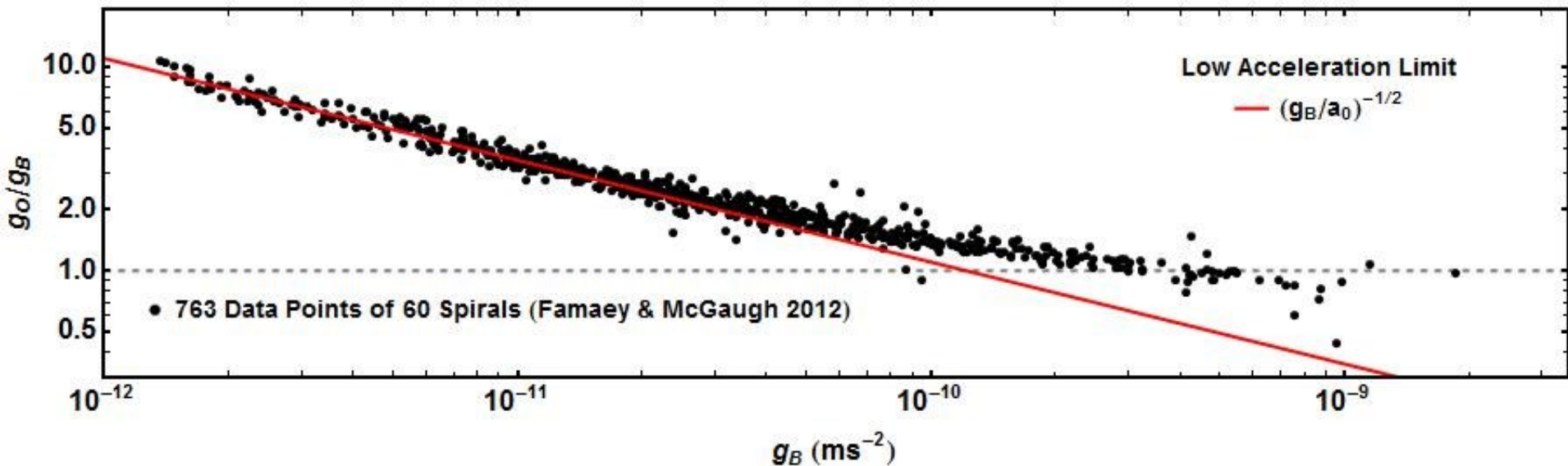


**Figure 11:** The mass-discrepancy–acceleration relation from Figure 10 extended to solar-system scales (each planet is labelled). This illustrates the large gulf in scale between galaxies and the Solar system where high precision tests are possible. The need for dark matter only appears at very low accelerations.

# Dynamics & Kinematics

	Dynamics	Kinematics
Solar System	Newtonian Laws	Kepler's Law
Spiral Galaxy	MDAR	Tully-Fisher Relation

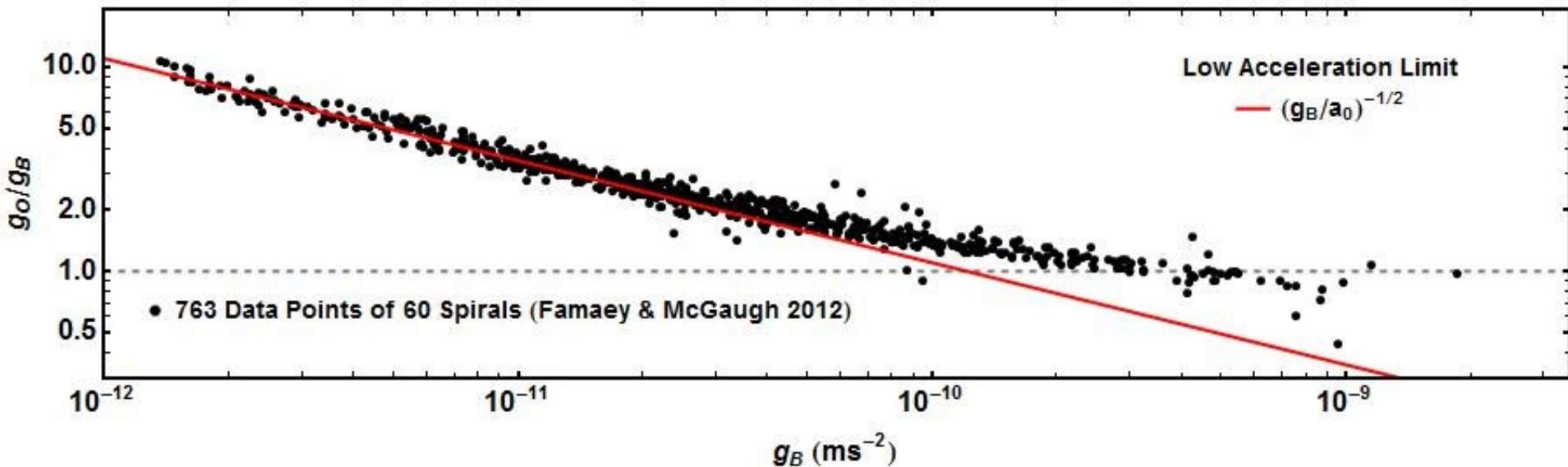
# Mass Discrepancy-Acceleration Relation: MDAR & Tully-Fisher Relation



$$\text{Log}_{10} \left[ \frac{g_o}{g_B} \right] = \frac{-1}{2} \text{Log}_{10}[g_B] + \frac{1}{2} \text{Log}_{10}[a_0]$$

$$g_o = (g_B a_0)^{1/2}$$

# Mass Discrepancy-Acceleration Relation: MDAR & Tully-Fisher Relation



$$g_o^2 = g_B a_0$$
$$g_o = \frac{v^2}{r}, \quad g_B = \frac{GM_B}{r^2}$$

$$\rightarrow \frac{v^4}{r^2} = \frac{GM_B a_0}{r^2}$$

$$\rightarrow v^4 = GM_B a_0$$

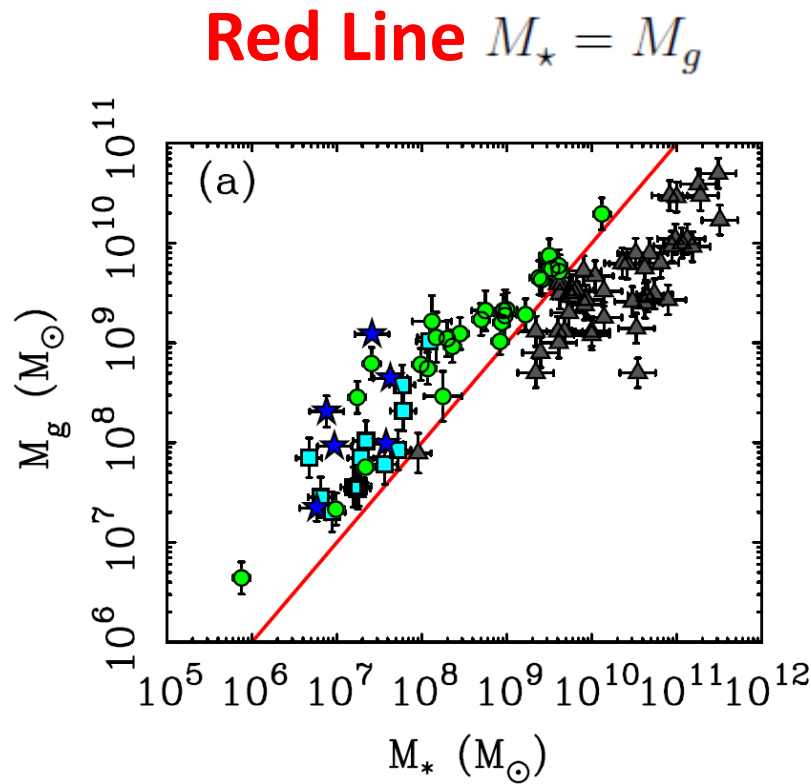
Baryonic Tully-Fisher Relation





# Novel Test of Modified Newtonian Dynamics with Gas Rich Galaxies

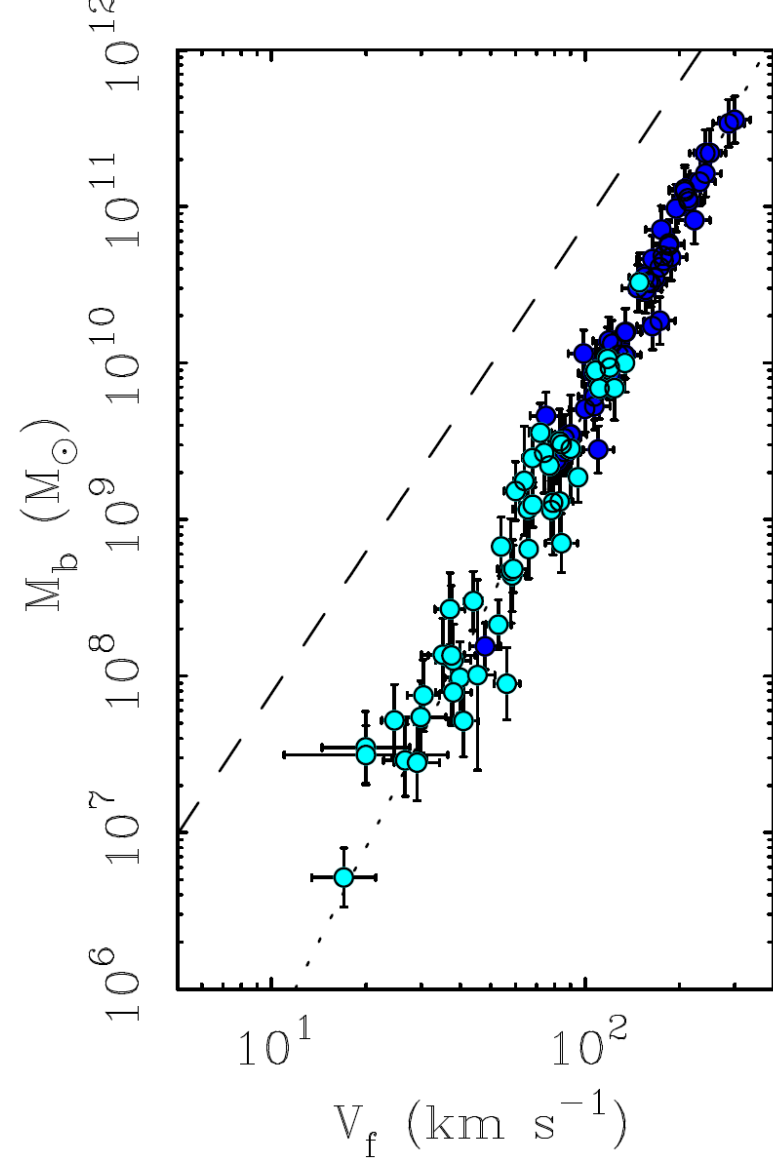
Stacy S. McGaugh



$$v^4 = GMa_0$$

Slope  $3.8 \pm 0.2$

$$a_0 = 1.24 \pm 0.14 \times 10^{-10} \text{ m s}^{-2}$$

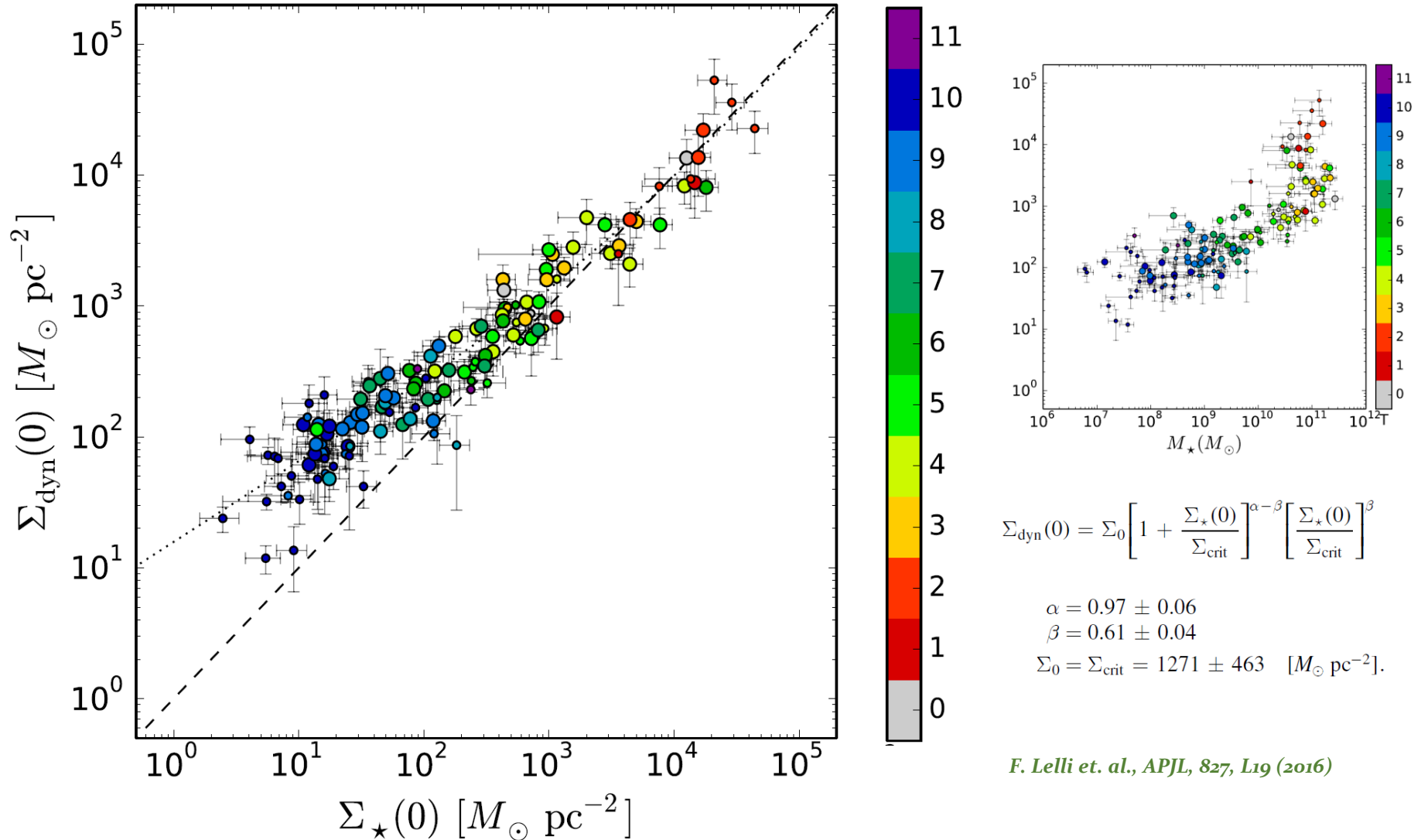




# THE RELATION BETWEEN STELLAR AND DYNAMICAL SURFACE DENSITIES IN THE CENTRAL REGIONS OF DISK GALAXIES

FEDERICO LELLI<sup>1</sup>, STACY S. MCGAUGH<sup>1</sup>, JAMES M. SCHOMBERT<sup>2</sup>, AND MARCEL S. PAWLOWSKI<sup>1</sup>

<sup>1</sup>Department of Astronomy, Case Western Reserve University, Cleveland, OH 44106, USA; [federico.elli@case.edu](mailto:federico.elli@case.edu)





# Radial Acceleration Relation in Rotationally Supported Galaxies

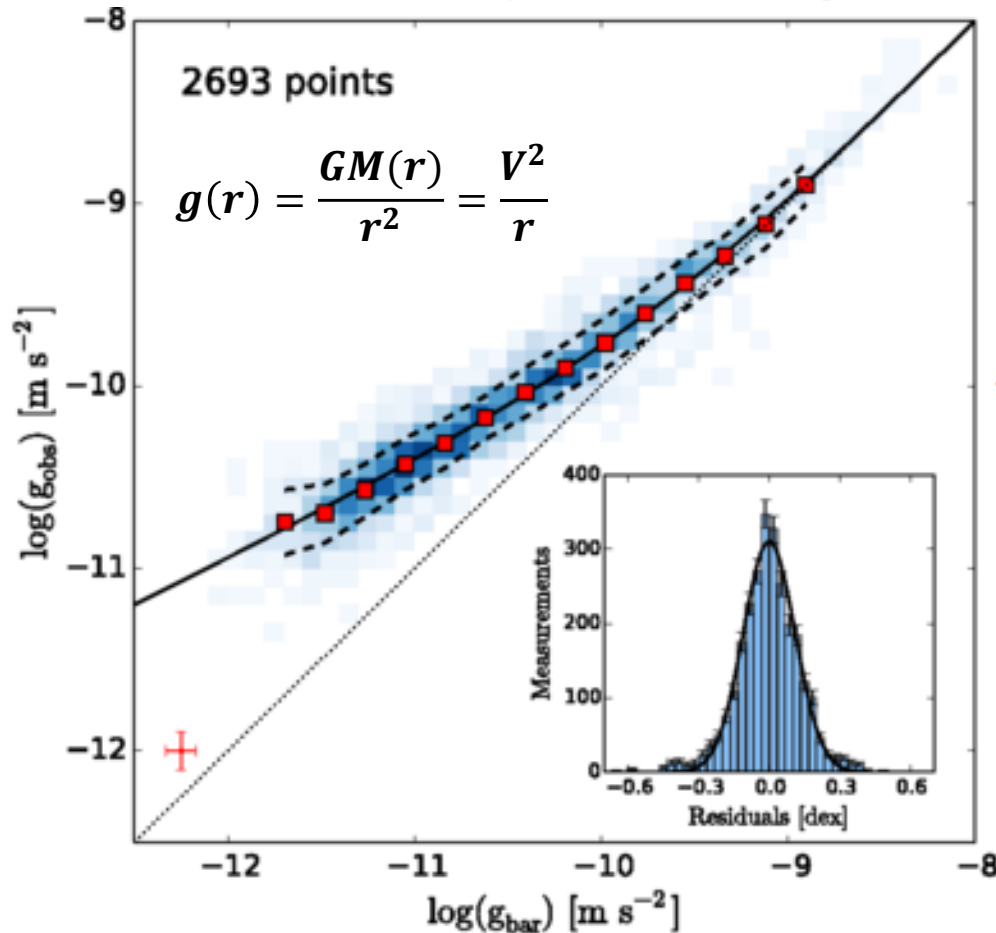
Stacy S. McGaugh and Federico Lelli

*Department of Astronomy, Case Western Reserve University, 10900 Euclid Avenue, Cleveland, Ohio 44106, USA*

James M. Schombert

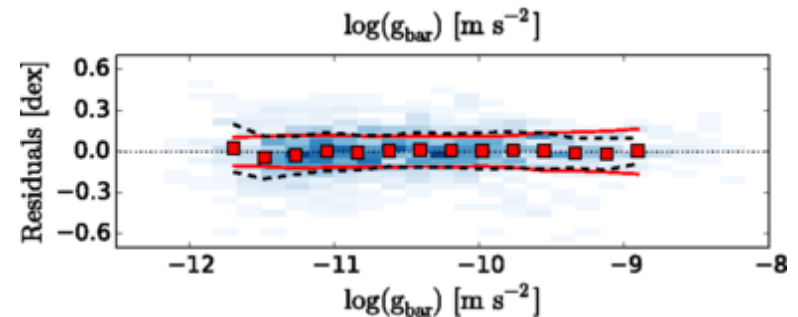
*Department of Physics, University of Oregon, Eugene, Oregon 97403, USA*

(Received 18 May 2016; revised manuscript received 7 July 2016; published 9 November 2016)



$$g_{\text{DM}} = g_{\text{obs}} - g_{\text{bar}} = \frac{g_{\text{bar}}}{e^{\sqrt{g_{\text{bar}}/g_{\dagger}} - 1}}$$

$$g_{\dagger} = 1.20 \pm 0.02 (\text{random}) \pm 0.24 (\text{syst}) \times 10^{-10} \text{ ms}^{-2}$$

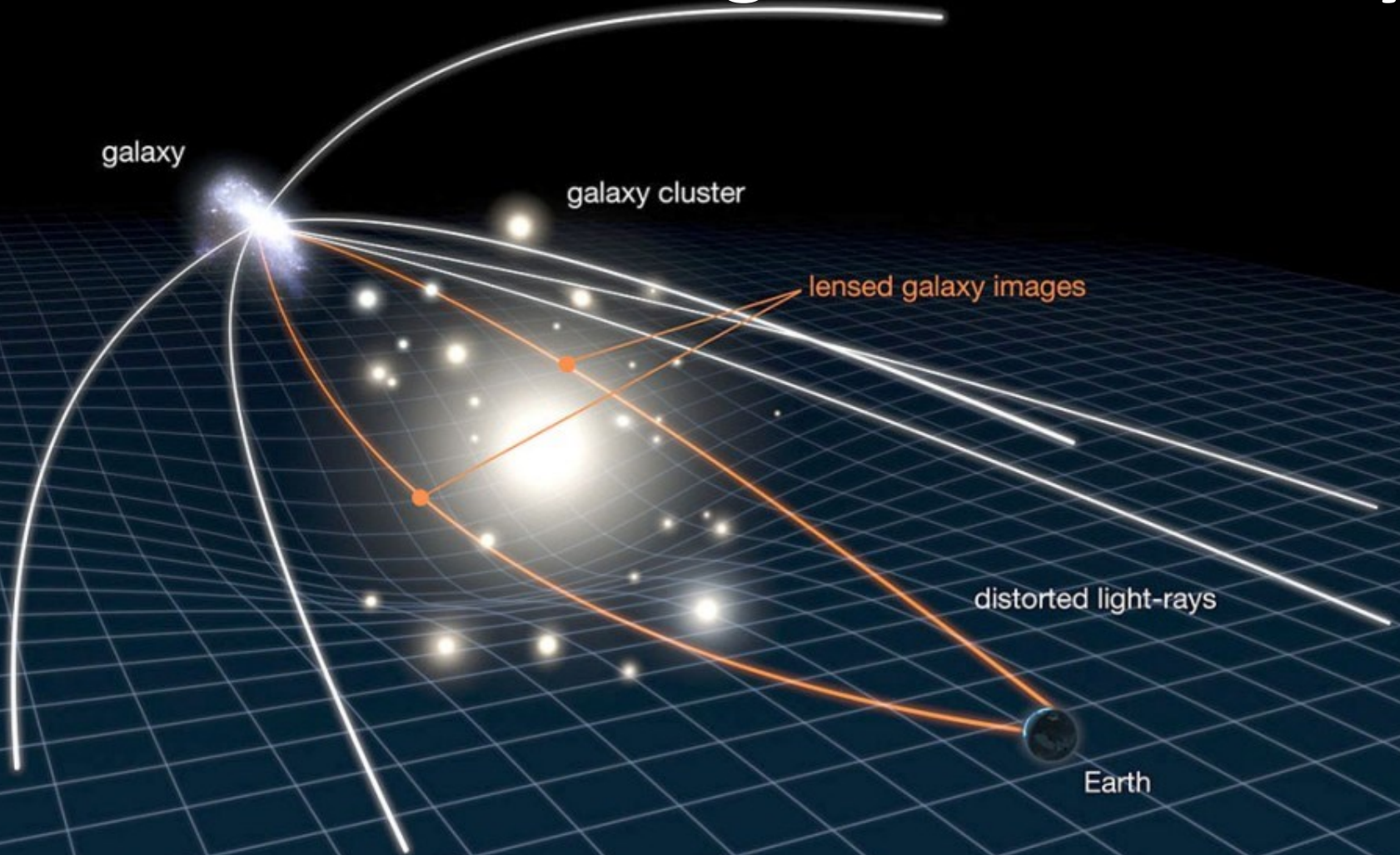


**MDAR in  
Elliptical Galaxies?**

**Dynamics? Lensing?**



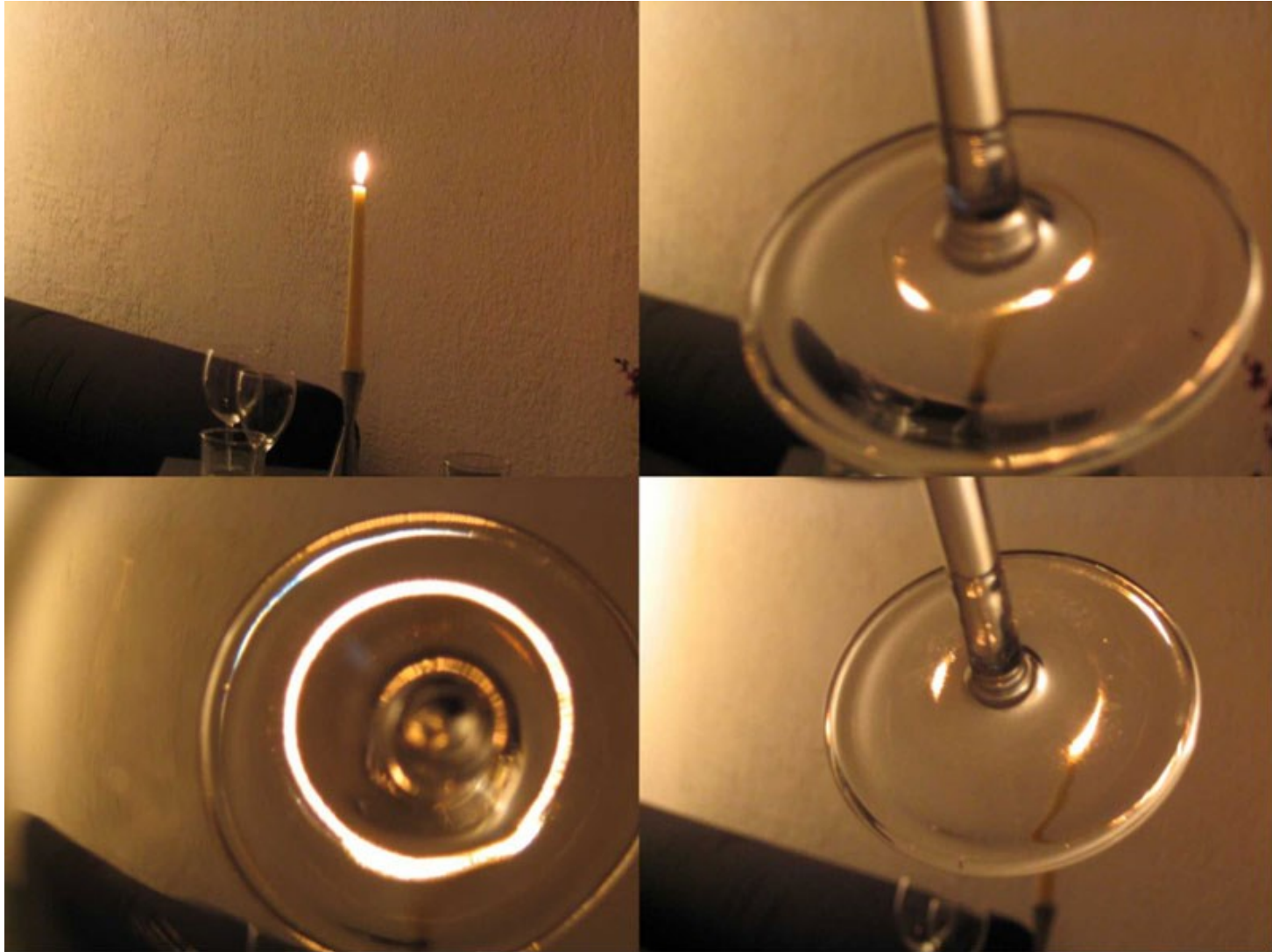
# Gravitational Lensing and Time Delay



**Lensing**  
**Bigger Deflection Angle**

**Time Delay**  
**Larger Hubble Constant**

# Introduction to Gravitational Lensing



Reference: Ann. Rev. Astron. Astrophys. 48 (2010) 87-125



# THE SLOAN LENS ACS SURVEY. IX. COLORS, LENSING, AND STELLAR MASSES OF EARLY-TYPE GALAXIES

M. W. AUGER<sup>1</sup>, T. TREU<sup>1,7</sup>, A. S. BOLTON<sup>2</sup>, R. GAVAZZI<sup>3</sup>, L. V. E. KOOPMANS<sup>4</sup>, P. J. MARSHALL<sup>1</sup>, K. BUNDY<sup>5,8</sup>, AND  
L. A. MOUSTAKAS<sup>6</sup>

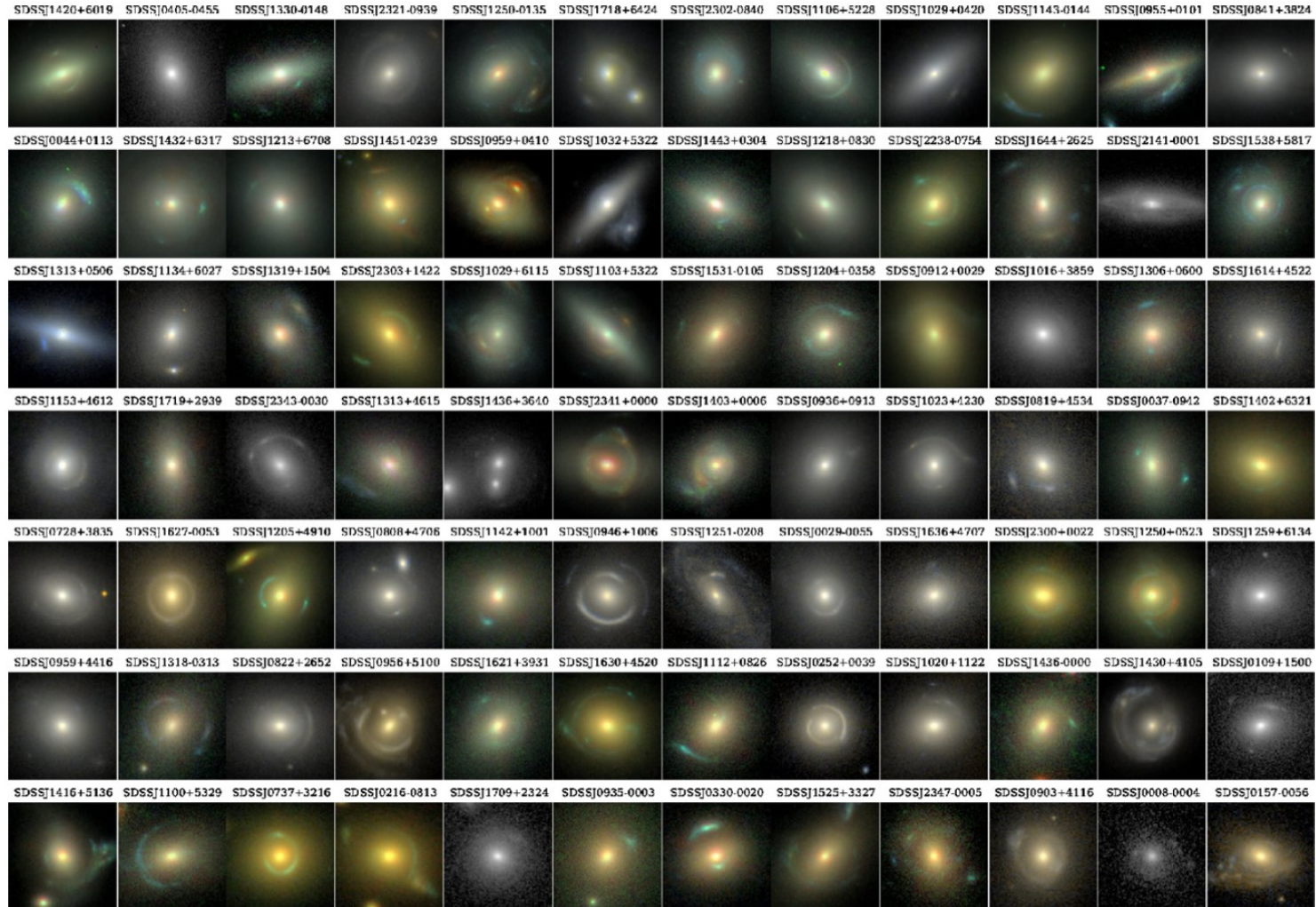


**Figure 2.** Color cutouts of 84 of the SLACS lenses, ordered by redshift. The lens SDSSJ1618+4353 has two primary lensing galaxies and has not been included.

# THE SLOAN LENS ACS SURVEY. IX. COLORS, LENSING, AND STELLAR MASSES OF EARLY-TYPE GALAXIES

M. W. AUGER<sup>1</sup>, T. TREU<sup>1,7</sup>, A. S. BOLTON<sup>2</sup>, R. GAVAZZI<sup>3</sup>, L. V. E. KOOPMANS<sup>4</sup>, P. J. MARSHALL<sup>1</sup>, K. BUNDY<sup>5,8</sup>, AND L. A. MOUSTAKAS<sup>6</sup>

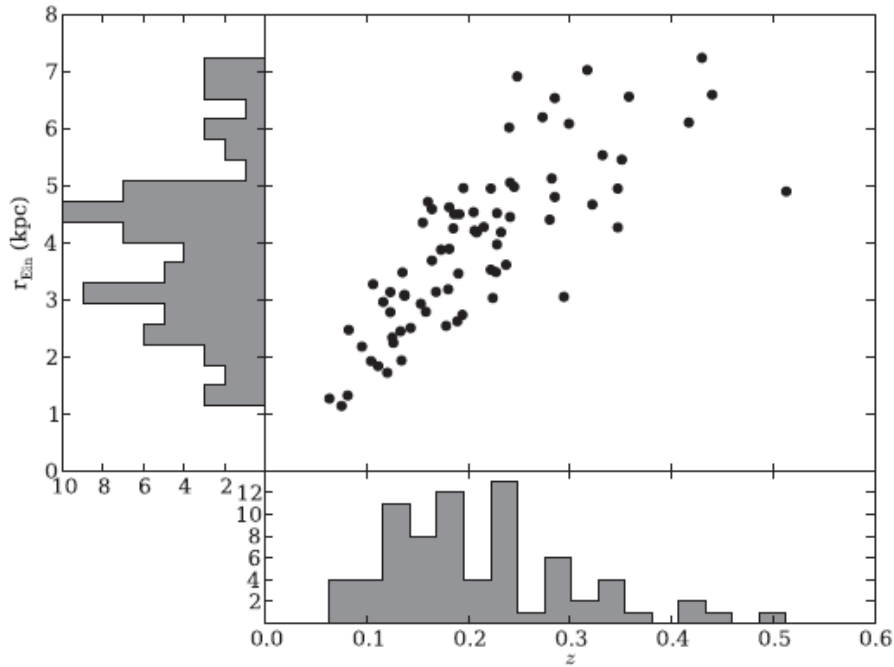


**Figure 7.** Redshift and Einstein radius,  $r_{\text{Ein}}$ , distributions for SLACS lenses. The median redshift is 0.19 and the median  $r_{\text{Ein}}$  is 4 kpc. There is a strong correlation between mass and redshift that results from the magnitude limit of the SDSS spectroscopic survey (see Figure 8).

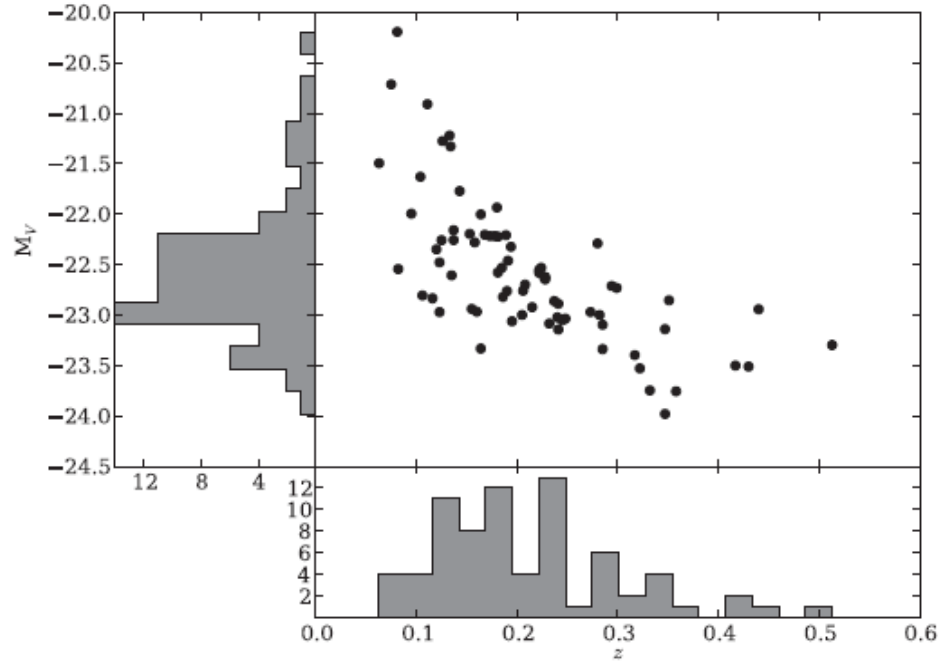


**Figure 8.** Redshift and magnitude distributions for SLACS lenses. The strong correlation between luminosity and redshift is the result of the selection function of the SLACS lenses, which are drawn from the magnitude-limited SDSS spectroscopic survey.

We select elliptical galaxy lenses with complete photometric data and estimation of stellar IMF mass. We also exclude S0 galaxies because of the mass model. As a result, we have 57 Einstein rings in our samples

# Mass discrepancy–acceleration relation in Einstein rings

Yong Tian<sup>1★</sup> and Chung-Ming Ko<sup>1,2★</sup>

<sup>1</sup>*Institute of Astronomy, National Central University, Taoyuan City, Taiwan 32001, Republic of China*

<sup>2</sup>*Department of Physics and Center for Complex Systems, National Central University, Taoyuan City, Taiwan 32001, Republic of China*

## ➤ Lensing Equation of Einstein Rings

$$\alpha(\theta) = \frac{2}{c^2} \int_{-\infty}^{\infty} \nabla_{\perp} \Phi \, ds, \quad \theta = \alpha(\theta) \frac{D_{\text{LS}}}{D_{\text{S}}},$$

## ➤ Hernquist Model for Baryonic Mass

$$m_{\text{b}}(r) = \frac{\mathcal{M}_{\text{Bar}} r^2}{(r + r_h)^2}, \quad g_{\text{b}}(r) = \frac{G \mathcal{M}_{\text{Bar}}}{(r + r_h)^2},$$

with  $r_h \approx 0.551 R_{\text{eff}}$ .

## ➤ Isothermal Model for Dark Matter Mass

$$g_{\text{iso}}(r) = \frac{2\sigma_v^2}{r}$$



# An extensive catalogue of early-type galaxies in the nearby Universe

J. Dabringhausen<sup>★</sup> and M. Fellhauer<sup>★</sup>

*Departamento de Astronomía, Universidad de Concepcion, Casilla 160-C, Concepcion, Chile*

## ABSTRACT

We present a catalogue of 1715 early-type galaxies from the literature, spanning the luminosity range from faint dwarf spheroidal galaxies to giant elliptical galaxies. The aim of this catalogue

**Table 11.** Structural properties and internal dynamics of the galaxies in this catalogue. A portion of the table is shown here for guidance regarding its contents and form. A detailed description of the contents of this table is given in Section 7.2. The table in its entirety can be downloaded at <http://www.astro-udec.cl/mf/catalogue/>.

id	$R_e$ (pc)	$dR_e$ (pc)	s.	$n$	$dn$	s.	$\sigma_e$ (km s <sup>-1</sup> )	$+d\sigma_e$ (km s <sup>-1</sup> )	$-d\sigma_e$ (km s <sup>-1</sup> )	s.	$\sigma_0$ (km s <sup>-1</sup> )	$+d\sigma_0$ (km s <sup>-1</sup> )	$-d\sigma_0$ (km s <sup>-1</sup> )	s.	$v_{rot}$ (km s <sup>-1</sup> )	$+dv_{rot}$ (km s <sup>-1</sup> )	$-dv_{rot}$ (km s <sup>-1</sup> )	s.	$M_{dyn}$ [lg( $M_\odot$ )]	$dM_{dyn}$ [lg( $M_\odot$ )]	s.
501	1879.9	188.0	1	2.8	0.4	1	75.7	3.8	3.8	1	76.7	3.8	3.8	1	58.3	-9.9	-9.9	1	9.75	0.09	1
502	2433.1	243.3	1	4.2	1.7	1	82.0	4.1	4.1	1	91.8	4.6	4.6	1	21.9	-9.9	-9.9	1	9.70	0.09	1
503	2043.4	204.3	1	8.4	2.0	1	128.5	6.4	6.4	1	132.4	6.6	6.6	1	36.2	-9.9	-9.9	1	10.23	0.09	1
504	6949.9	-9.9	2	5.2	2.2	0	267.3	-9.9	-9.9	101	290.4	-9.9	-9.9	2	-9.9	-9.9	-9.9	0	11.68	-99.99	101
505	2393.8	239.4	1	4.4	0.4	1	62.2	3.1	3.1	1	56.2	2.8	2.8	1	8.5	-9.9	-9.9	1	9.65	0.09	1

**Table 15.** Stellar populations of the galaxies in this catalogue. A portion of the table is shown here for guidance regarding its contents and form. A detailed description of the contents of this table is given in Section 8.2. The table in its entirety can be downloaded at <http://www.astro-udec.cl/mf/catalogue/>.

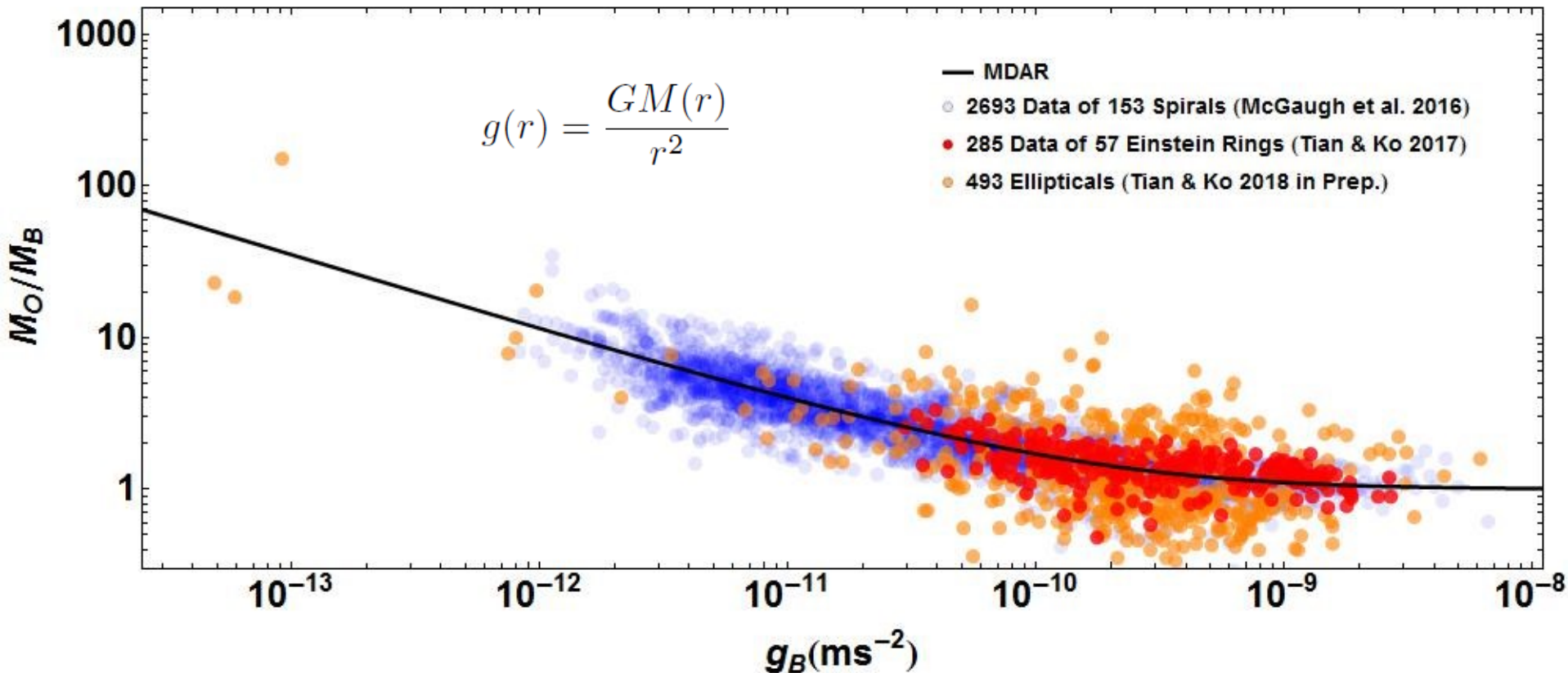
id	$t$ (Gyr)	$+dt$ (Gyr)	$-dt$ (Gyr)	s.	[Z/H]	$+d[Z/H]$	$-d[Z/H]$	s.	$M_s$ lg( $M_\odot$ )	$dM_s$ lg( $M_\odot$ )	s.
501	3.5	0.6	0.6	1	-0.38	0.06	0.06	1	9.81	-99.99	1011
502	1.0	0.1	0.1	1	0.18	0.06	0.06	1	9.68	-99.99	1011
503	9.7	1.6	1.6	1	-0.36	0.05	0.05	1	10.09	-99.99	1011
504	-9.9	-9.9	-9.9	0	0.06	99.99	99.99	1020	11.46	-99.99	1020
505	2.5	0.3	0.3	1	-0.78	0.06	0.06	1	9.18	-99.99	1011

# Mass discrepancy–acceleration relation in Einstein rings

Yong Tian<sup>1★</sup> and Chung-Ming Ko<sup>1,2★</sup>

<sup>1</sup>*Institute of Astronomy, National Central University, Taoyuan City, Taiwan 32001, Republic of China*

<sup>2</sup>*Department of Physics and Center for Complex Systems, National Central University, Taoyuan City, Taiwan 32001, Republic of China*

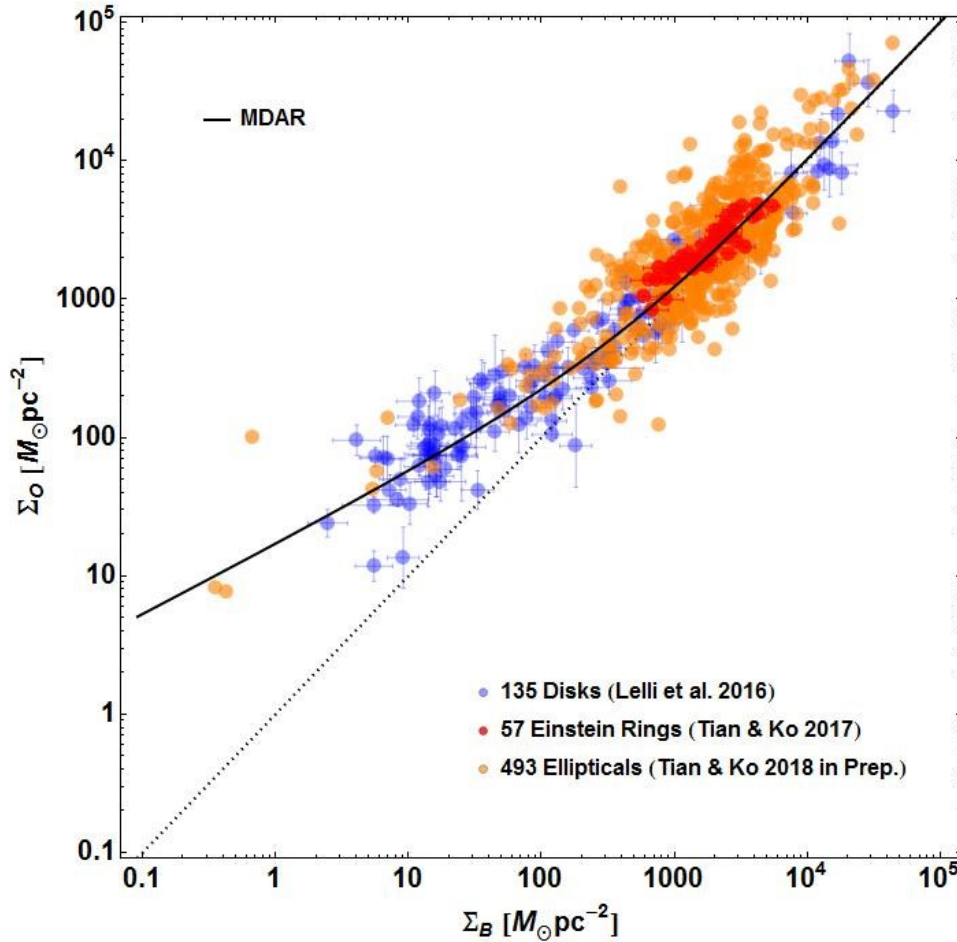


# Mass discrepancy–acceleration relation in Einstein rings

Yong Tian<sup>1★</sup> and Chung-Ming Ko<sup>1,2★</sup>

<sup>1</sup>*Institute of Astronomy, National Central University, Taoyuan City, Taiwan 32001, Republic of China*

<sup>2</sup>*Department of Physics and Center for Complex Systems, National Central University, Taoyuan City, Taiwan 32001, Republic of China*



$$\Sigma = \frac{M}{\pi r^2} \approx \frac{a}{G}$$

$$\Sigma_0 \equiv \frac{a_0}{G} = 276 M_{\odot} pc^{-2}$$



## Radial Acceleration Relation in Rotationally Supported Galaxies

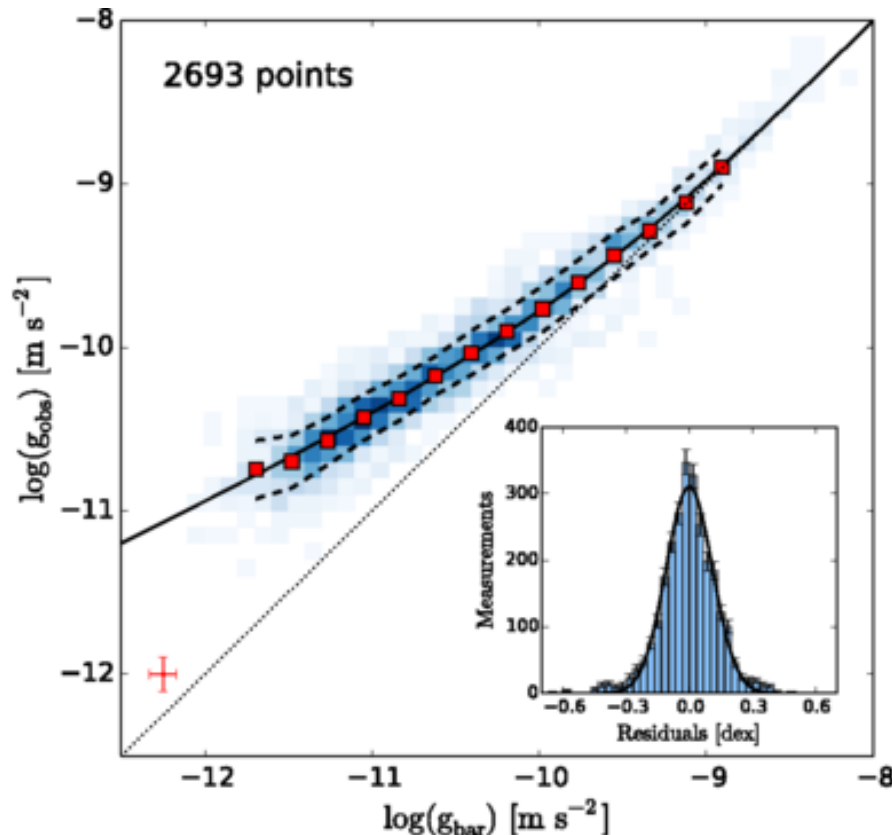
Stacy S. McGaugh and Federico Lelli

*Department of Astronomy, Case Western Reserve University, 10900 Euclid Avenue, Cleveland, Ohio 44106, USA*

James M. Schombert

*Department of Physics, University of Oregon, Eugene, Oregon 97403, USA*

(Received 18 May 2016; revised manuscript received 7 July 2016; published 9 November 2016)

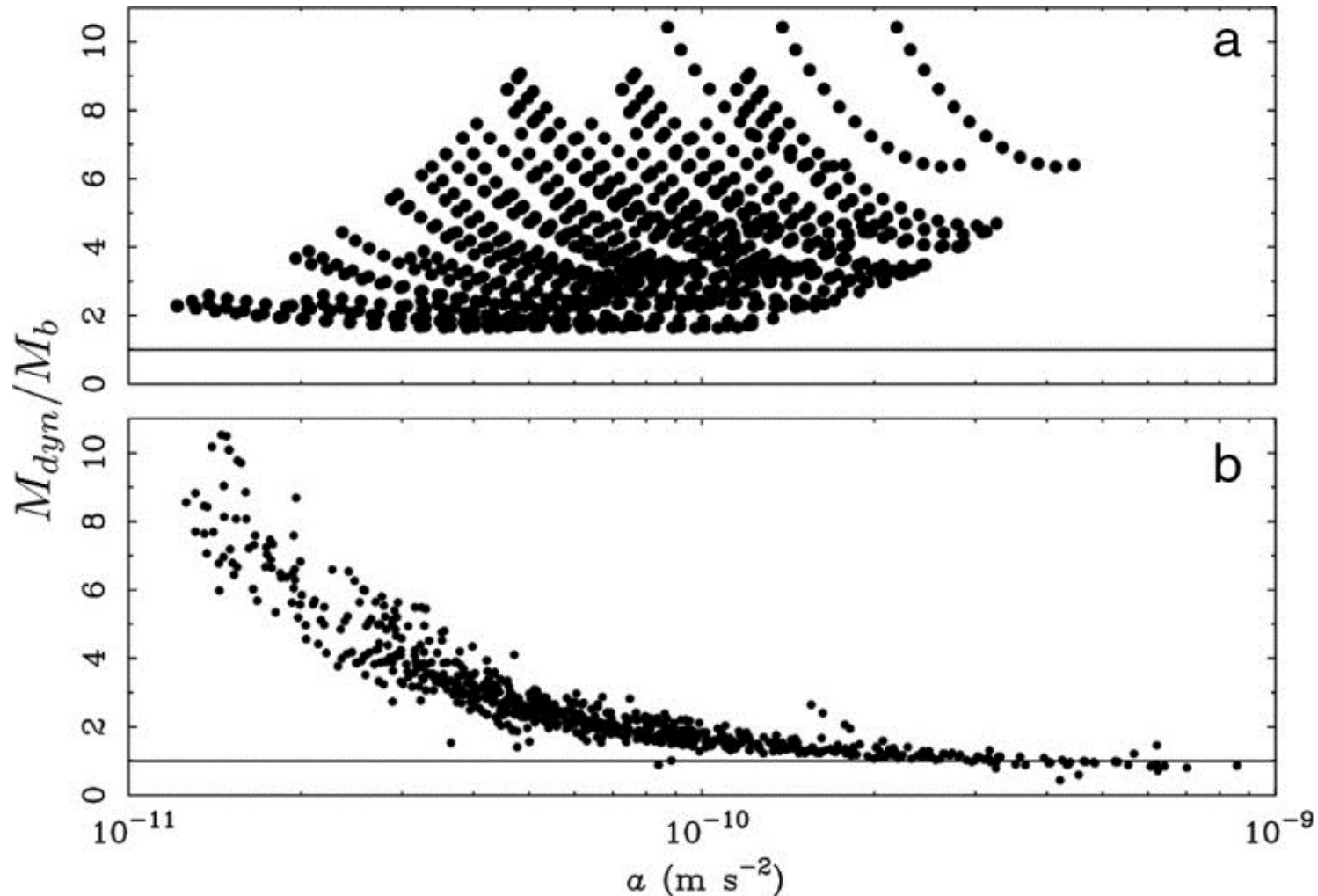


### Three implications

1. New “Dark Sector” physics
2. The result of galaxy formation
3. New dynamics law

# A tale of two paradigms: the mutual incommensurability of $\Lambda$ CDM and MOND<sup>1</sup>

Stacy S. McGaugh







# Mass-Discrepancy Acceleration Relation: A Natural Outcome of Galaxy Formation in Cold Dark Matter Halos

Aaron D. Ludlow,<sup>\*</sup> Alejandro Benítez-Llambay, Matthieu Schaller, Tom Theuns,  
Carlos S. Frenk, and Richard Bower  
*Institute for Computational Cosmology, Department of Physics, Durham University,  
Durham DH1 3LE, United Kingdom*

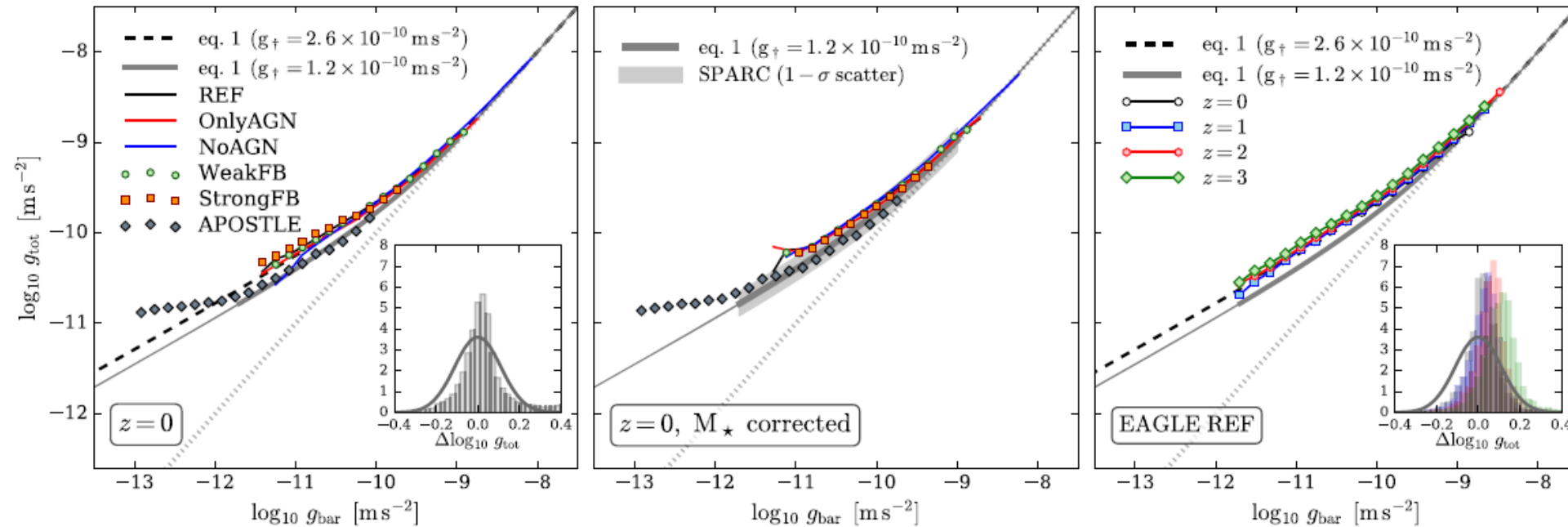


FIG. 3. Total acceleration profiles for all halos as a function of their baryonic acceleration. The left panel shows results for all halos in all simulations at  $z = 0$ . Lines, points, and colors have the same meaning as in Fig. 1. The right-hand panel shows (for REF) the redshift evolution for progenitor galaxies. The dashed lines in the left- and right-hand panels show Eq. (1) with  $g_{\dagger} = 2.6 \times 10^{-10} \text{ m s}^{-2}$ . Inset panels show the relative scatter around this curve after combining all simulations (left) and for individual redshifts (right); the solid lines represent the observational scatter in Ref. [15]. The middle panel plots the  $g_{\text{obs}} - g_{\text{bar}}$  relation after rescaling galaxy stellar masses so that they fall on the abundance matching relation shown in Fig. 1 (left). The thick gray line and shaded band indicate the mean trend and scatter, respectively, obtained by Ref. [15] from observations of rotationally supported galaxies.



# A MODIFICATION OF THE NEWTONIAN DYNAMICS AS A POSSIBLE ALTERNATIVE TO THE HIDDEN MASS HYPOTHESIS<sup>1</sup>

M. MILGROM

Department of Physics, The Weizmann Institute of Science, Rehovot, Israel; and  
The Institute for Advanced Study

*Received 1982 February 4; accepted 1982 December 28*

***Poisson's Equation – The differential form of Gauss's law of gravity***

$$\nabla \cdot g_B = -4\pi G\rho$$

***Modified Poisson's Equation***

$$\nabla \cdot (\mu(g_0/a_0)g_0) = -4\pi G\rho$$

***where  $\mu(x)$  has the asymptotic behaviour and***

$$a_0 = 1.2 \times 10^{-10} \text{ms}^{-2}$$

$$\mu(x) \approx 1 \text{ for } x \gg 1, \quad \mu(x) \approx x \text{ for } x \ll 1$$

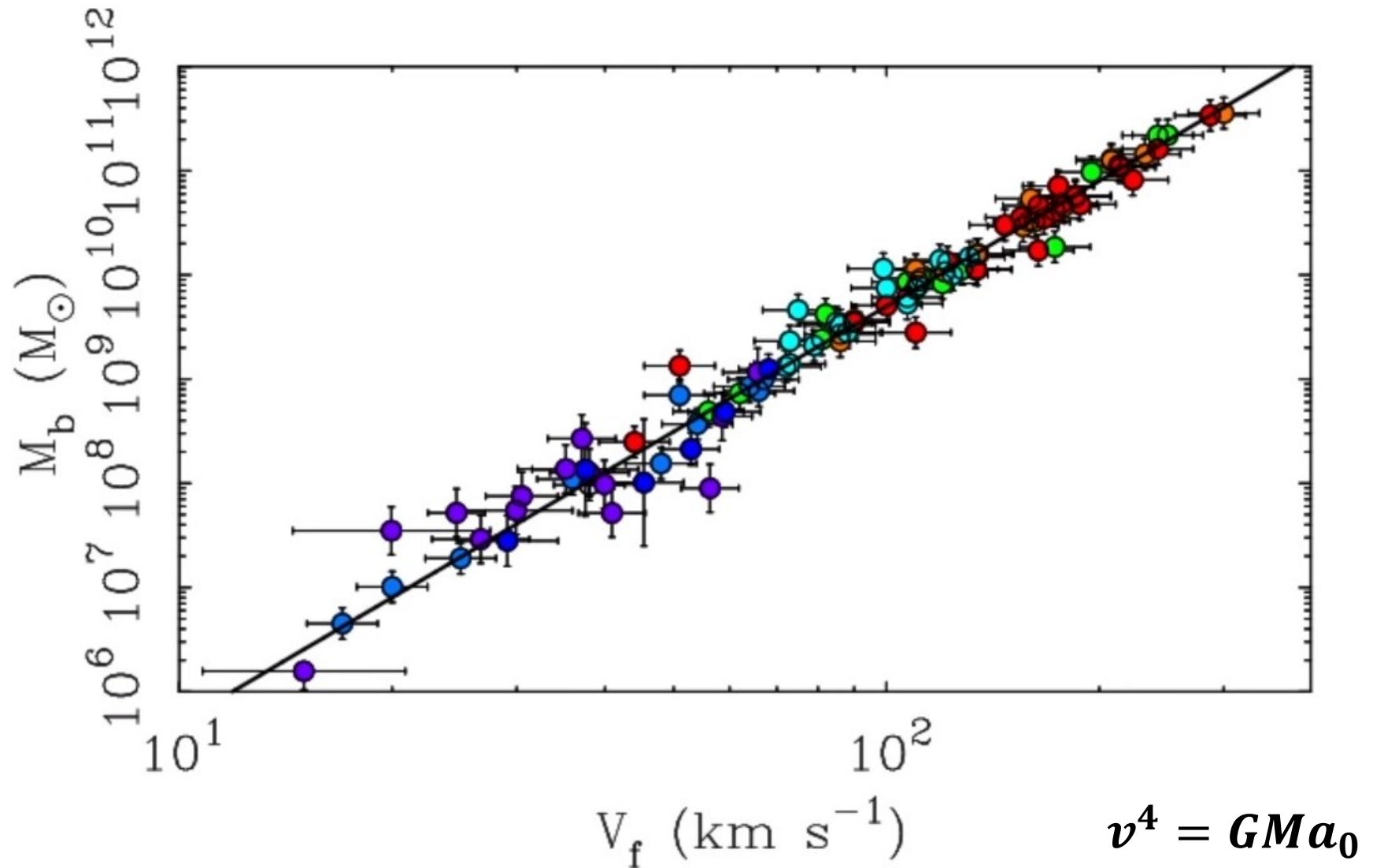
***Thus,***

$$\mu(g_0/a_0) \cdot g_0 = g_B$$

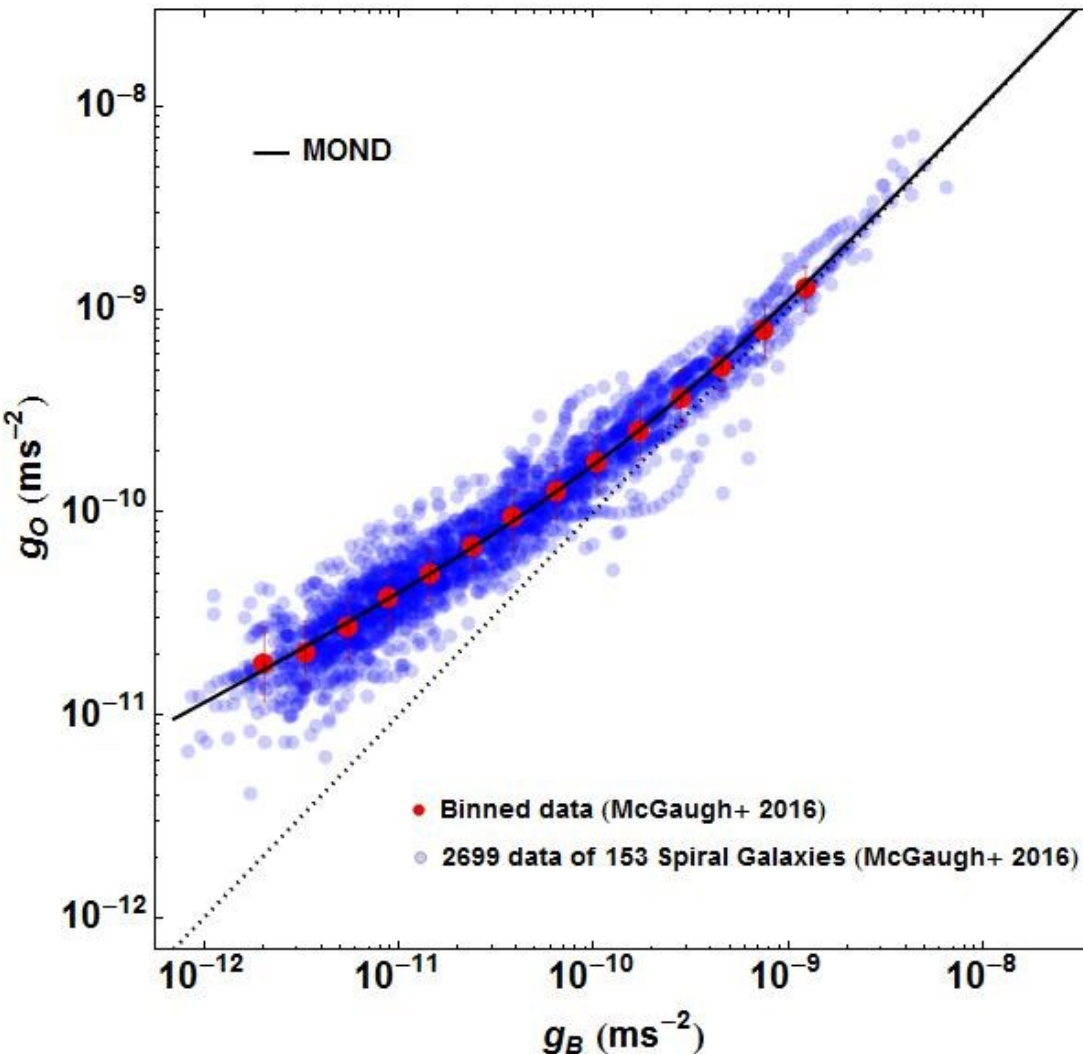
***For low acceleration,***  $(g_0/a_0) \cdot g_0 = g_B \rightarrow g_0 = (g_B a_0)^{\frac{1}{2}}$

***We can recover Tully – Fisher Relation,  $v^4 = GMa_0$***

# MOND and Tully-Fisher Relation



# MOdified Newtonian Dynamics (MOND)



Modified Newtonian Dynamics (MOND)

$$\frac{g_O}{g_B} = \nu\left(\frac{g_B}{a_0}\right)$$

where  $a_0 = 1.2 \times 10^{-10} \text{ms}^{-2}$

$\nu(y)$  has the asymptotic behaviour

$$\nu(y) \approx 1 \text{ for } y \gg 1$$

$$\nu(y) \approx y^{-1/2} \text{ for } y \ll 1$$

# Problem in MOND – Cluster of Galaxies

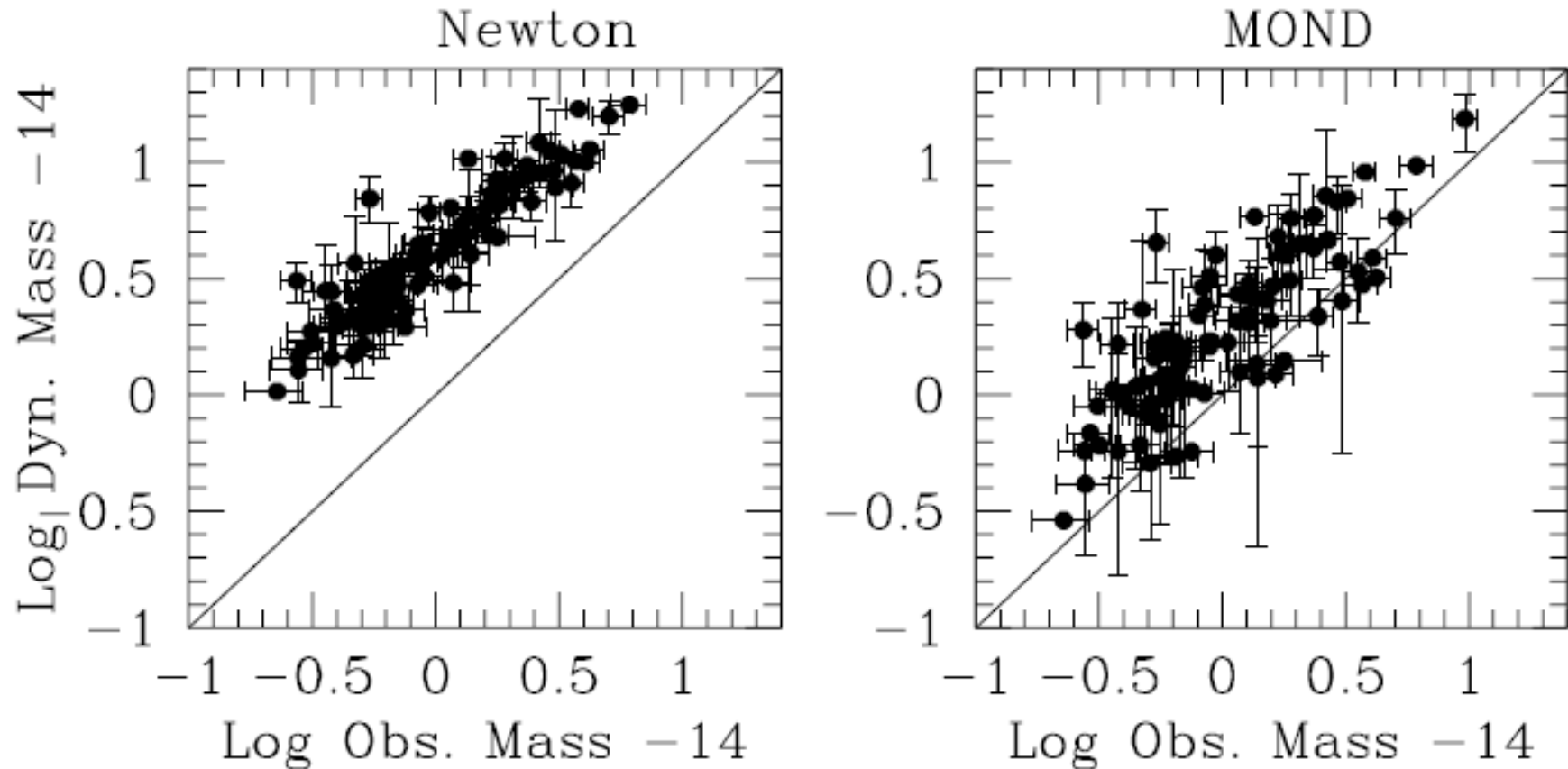


Figure 2.5: **Mass in Cluster of Galaxies in Newtonian and MONDian Dynamics.** *Left Panel:* the Newtonian dynamical mass in clusters of galaxies within an observed cutoff radius ( $r_{out}$ ) vs. the total observable mass in 93 X-ray emitting clusters of galaxies (White et al. (1997)). The solid line corresponds to  $M_{dyn} = M_{obs}$  (no discrepancy). *Right Panel:* the MOND dynamical mass within  $r_{out}$  vs. the total observable mass for the same X-ray emitting clusters from Sanders (1999); Sanders & McGaugh (2002).

*R.H. Sanders & S.S. McGaugh, ARAA, 40:263-317 (2002)*

# Bullet Cluster 1E 0657-558

- Clowe et al. 2006 claims the direct evidence of dark matter in Bullet Cluster 1E 0657-558
- X-ray image shows hot gas represents most of the baryon mass.
- Weak lensing contour did not match with hot gas.

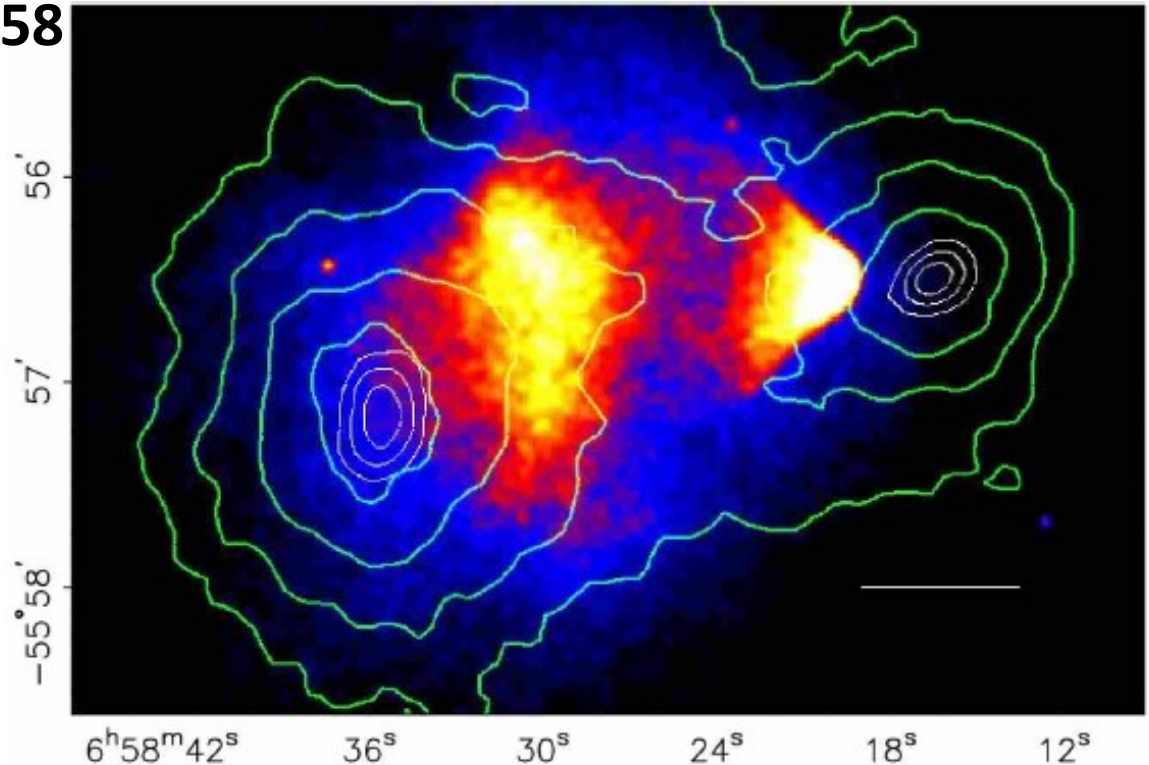


Figure 1.6: **Bullet Cluster 1E 0657–558.** *Top Panel:* Optical image of Bullet Cluster 1E0657–558 from the Magellan. Two blue plus signs “+” show the center of hot gas. White bar indicates 200 kpc. *Bottom Panel:* Chandra X-ray image of hot gas with Weak lensing mass contours (green and white line). (Clowe et al. (2006))

# Relativistic Problem & MOND

- ◆ MOND is the modification of weak field limit (g for static and localized system)
- ◆ MOND in relativistic DM problem needs the relativistic gravitational theory to explain.

**Ex.**

- **Gravitational Lensing**

- ☐ Strong Lensing – Quasar Lensing, time delay, Einstein rings
- ☐ Weak Lensing – Bullet Cluster

- **Large Scale Structure**

- **Cosmic Microwave Background Radiation (CMB)**



# The modified Newtonian law in relativistic theory?

## ➤ Bimetric Theory

Physical metric is deviated from Einstein metric by coupling additional fields.

## ➤ Additional fields (scalar, vector, tensor, etc.)

- The additional fields have their field equations.
- In weak field limit, these change the gravitational law.

**Relativistic gravitation theory for the modified Newtonian dynamics paradigm**Jacob D. Bekenstein<sup>\*,†</sup>*Racah Institute of Physics, Hebrew University of Jerusalem, Givat Ram, Jerusalem 91904 Israel*

(Received 29 March 2004; published 13 October 2004)

$$\tilde{g}^{\alpha\beta} = e^{2\phi} g^{\alpha\beta} + 2\mathfrak{U}^\alpha \mathfrak{U}^\beta \sinh(2\phi)$$

$$S_g = (16\pi G)^{-1} \int g^{\alpha\beta} R_{\alpha\beta} (-g)^{1/2} d^4x.$$

$$S_s = -\frac{1}{2} \int \left[ \sigma^2 h^{\alpha\beta} \phi_{,\alpha} \phi_{,\beta} + \frac{1}{2} G \ell^{-2} \sigma^4 F(kG\sigma^2) \right] (-g)^{1/2} d^4x,$$

$$\text{where } h^{\alpha\beta} \equiv g^{\alpha\beta} - \mathfrak{U}^\alpha \mathfrak{U}^\beta$$

$$S_v = -\frac{K}{32\pi G} \int \left[ g^{\alpha\beta} g^{\mu\nu} \mathfrak{U}_{[\alpha,\mu]} \mathfrak{U}_{[\beta,\nu]} - 2(\lambda/K)(g^{\mu\nu} \mathfrak{U}_\mu \mathfrak{U}_\nu + 1) \right] (-g)^{1/2} d^4x,$$

$$S_m = \int \mathcal{L}(\tilde{g}_{\mu\nu}, f^\alpha, f^\alpha|_{\mu}, \dots) (-\tilde{g})^{1/2} d^4x,$$

# Relativistic MOND

- **TeVSeS: Tensor-Vector-Scalar Theory (Bekenstein 2004)**
- **GEA: Generalized Einstein-Aether Theory (Zlosnik et al. 2007)**
- **BiMOND: Bimetric MOND Theory (Milgrom 2009)**
  
- **Gravitational lensing Test –**
  - Baryonic mass inferred from lensing is consistent to IMF mass. (Chu, Ko, **Tian**, and Zhao 2011, PRD)
  - Hubble constant is consistent with local value from Quasar time delay. (**Tian** et al. 2013, APJ)

# Summary

Relativistic Effect – 57 Elliptical Lens

Non-Relativistic Effect – 153 Spirals, 493 Ellipticals

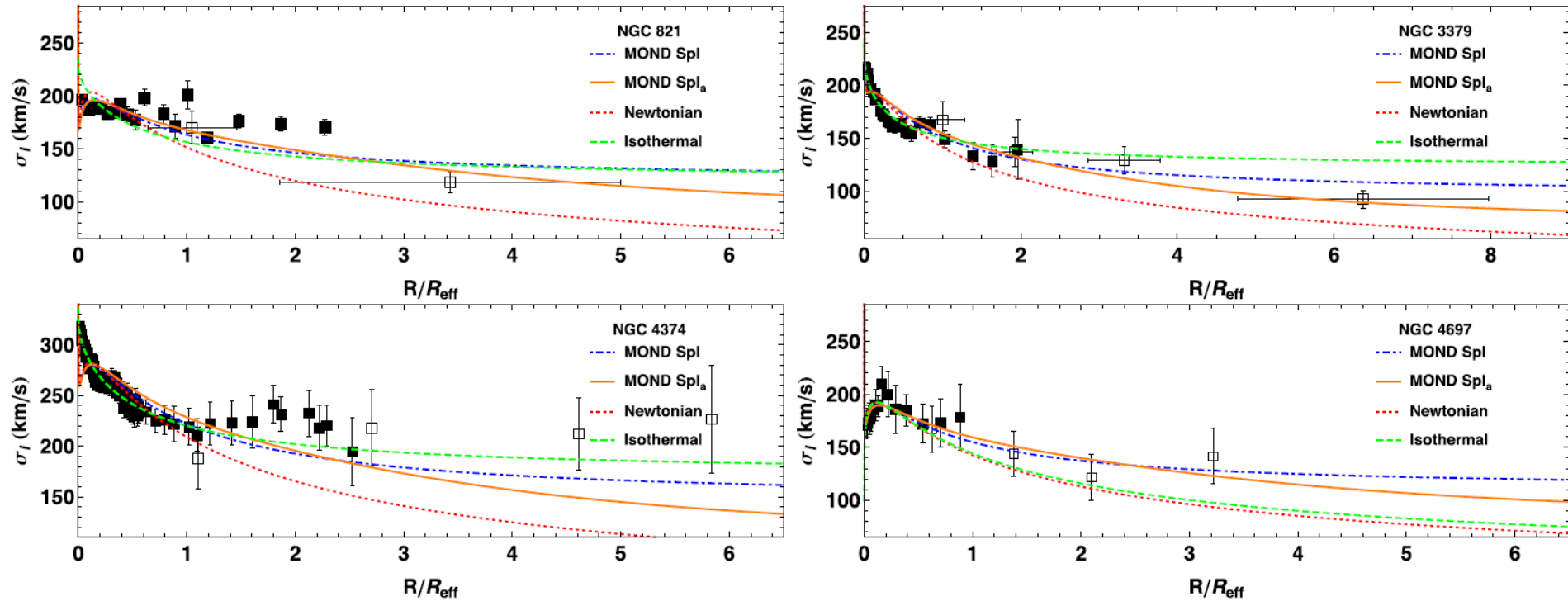
- The mass discrepancy (“missing mass” problem) can be represented as the acceleration relation.
- The **Mass Discrepancy-Acceleration Relation (MDAR)** can explain Baryonic Tully-Fisher relation.
- The MDAR of 57 Einstein Rings is consistent with 153 spiral galaxies (**Tian** & Ko 2017).
- The surface density relation between lensing surface and baryonic surface density is consistent to 135 disks (**Tian** & Ko 2018 in prep.)

**Thank You  
for Attention!**



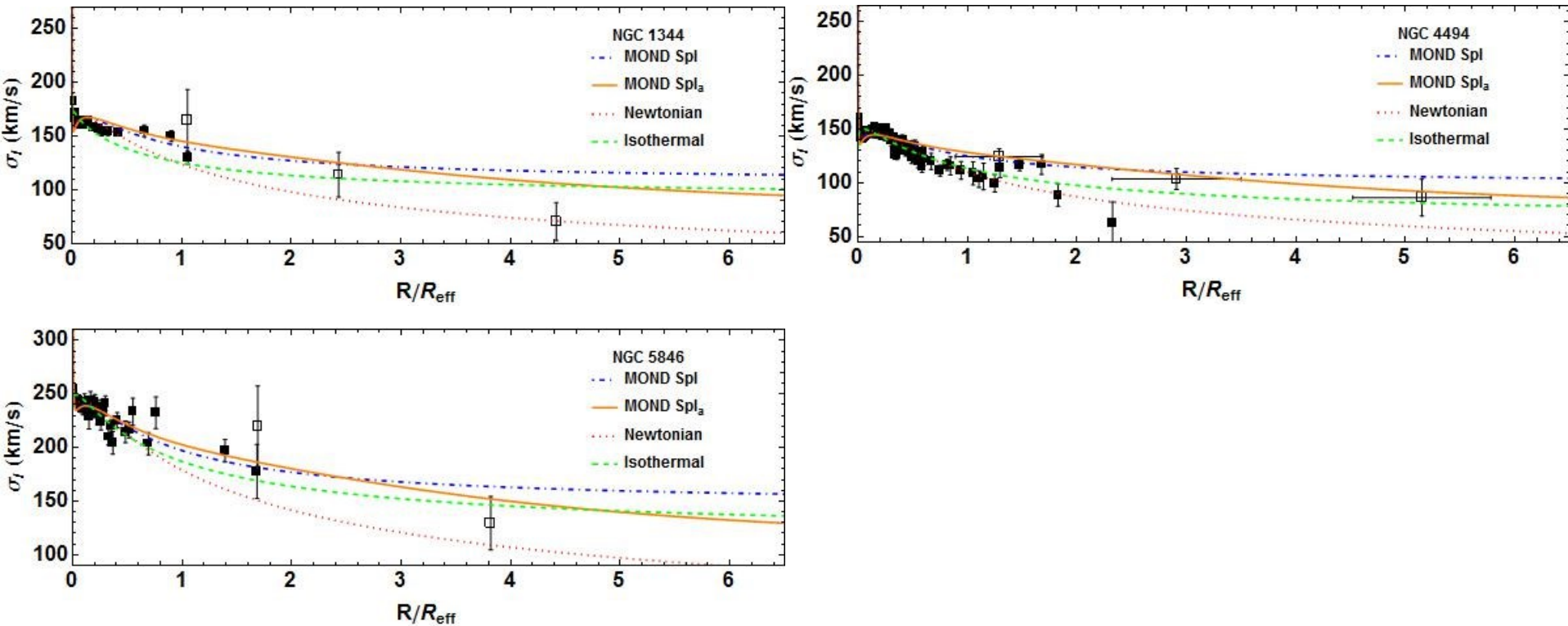
# Dynamics of elliptical galaxies with planetary nebulae in modified Newtonian dynamics

Yong Tian<sup>1★</sup> and Chung-Ming Ko<sup>1,2★</sup>



# Dynamics of elliptical galaxies with planetary nebulae in modified Newtonian dynamics

Yong Tian<sup>1★</sup> and Chung-Ming Ko<sup>1,2★</sup>



# Modified Newtonian Gravity Law?

In Newtonian dynamics, we have

$$g_O = g_B$$

$$\rightarrow \frac{v^2}{r} = \frac{GM_B}{r^2}$$

If we assume the gravity law change at large distance,

$$\frac{v^2}{r} = GM_B \left( \frac{1}{r^2} + \frac{1}{r} \right)$$

However, this leads problem of conservation law.

Thus, Milgrom in 1983 considered the modification of Newtonian's second law.

$$\mu(g_O/a_0)g_O = g_B$$

# GEA: Generalized Einstein-Aether Theory

*proposed by Zlosnik et al. in 2007*

$$S_g = (16\pi G)^{-1} \int g^{\alpha\beta} R_{\alpha\beta} (-g)^{1/2} d^4x$$

$$S_U = \frac{-c^4}{16\pi G l^2} \int [F(X_{GEA}) - l^2 \lambda (g^{\mu\nu} U_\mu U_\nu)] (-g)^{1/2} d^4x$$

$$X_{GEA} := l^2 K^{\alpha\beta\mu\nu} U_{\beta,\alpha} U_{\nu,\mu} ,$$

$$K^{\alpha\beta\mu\nu} := c_1 g^{\alpha\mu} g^{\beta\nu} + c_2 g^{\alpha\beta} g^{\mu\nu} + c_3 g^{\alpha\nu} g^{\beta\mu} + c_4 U^\alpha U^\mu g^{\beta\nu}$$

$$l \equiv \frac{3(2 - C)c^2}{2a_0 C^{3/2}}$$

# BiMOND: Bimetric MOND Theory

*proposed by Milgrom in 2009*

$$S = \frac{c^4}{16\pi G} \int [R - \hat{R} - 2l^{-2}F(X_{BiMOND})](-g)^{1/2}d^4x$$

$$l = c^2/\mathfrak{a}_0$$

$$X_{BiMOND} := l^2 g^{\mu\nu} (C_{\mu\beta}^{\alpha} C_{\nu\alpha}^{\beta} - C_{\mu\nu}^{\alpha} C_{\beta\alpha}^{\beta})$$

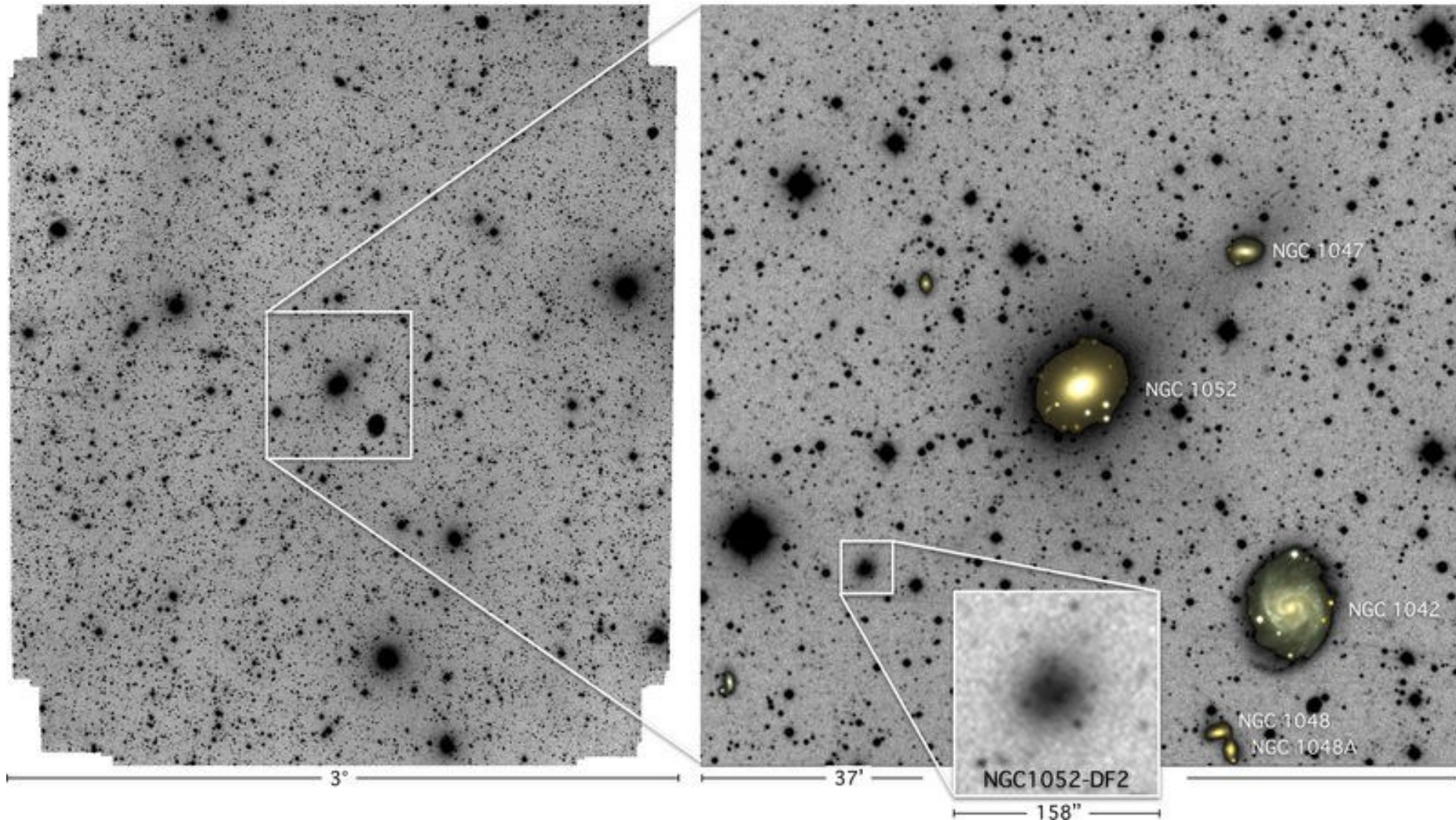
$$C_{\mu\nu}^{\alpha} = \Gamma_{\mu\nu}^{\alpha} - \hat{\Gamma}_{\mu\nu}^{\alpha}$$

$$\nabla^2 \Phi = 4\pi G \rho + \nabla \cdot [F'(|\nabla(\Phi - \hat{\Phi})|^2/\mathfrak{a}_0^2) \nabla(\Phi - \hat{\Phi})]$$

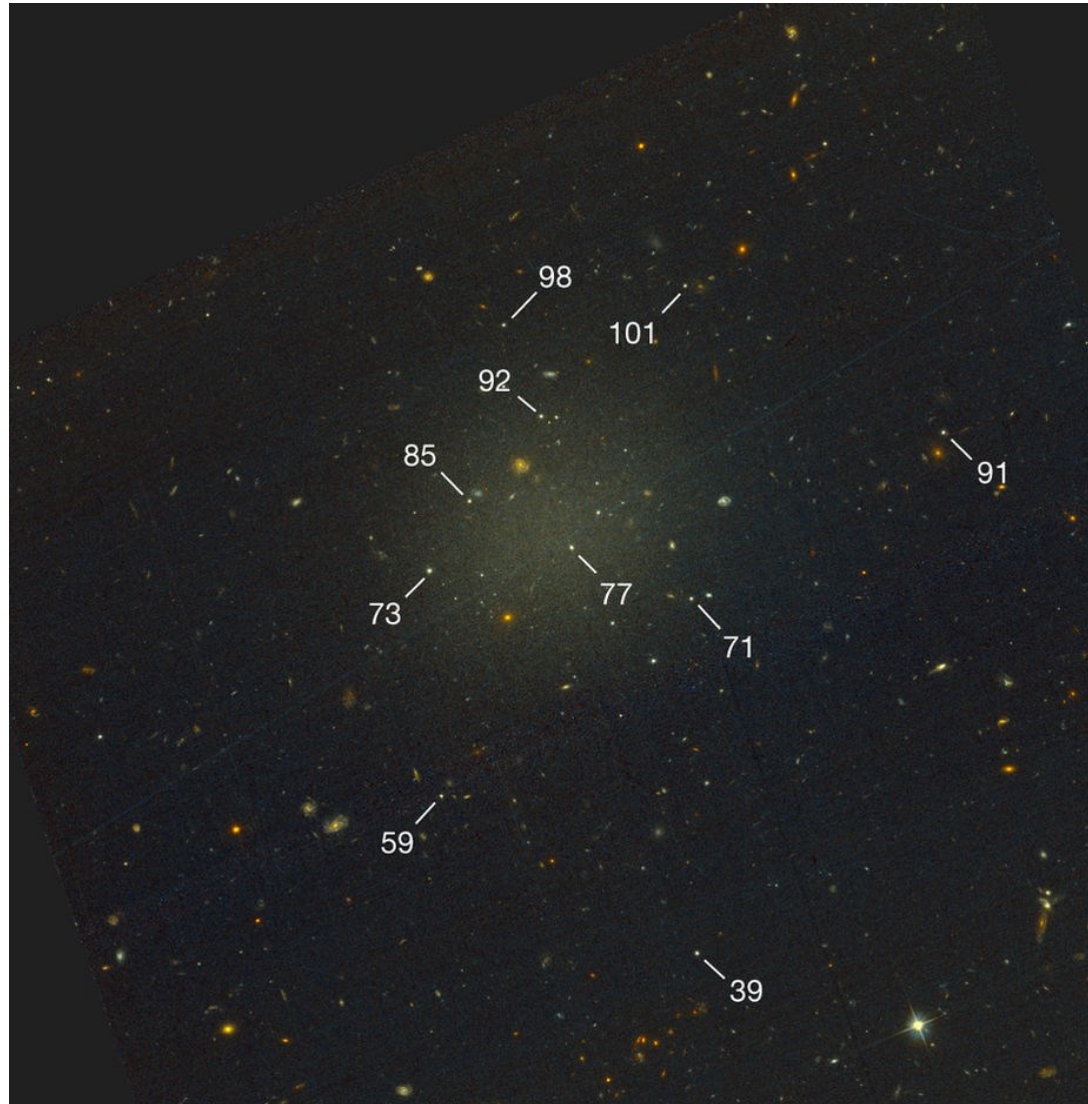
$$\nabla^2 \hat{\Phi} = 4\pi G \hat{\rho} + \nabla \cdot [F'(|\nabla(\Phi - \hat{\Phi})|^2/\mathfrak{a}_0^2) \nabla(\Phi - \hat{\Phi})]$$



# Ultra-Diffuse Galaxy (UDG) - NGC1052-DF2



# Ultra-Diffuse Galaxy (UDG) - NGC1052–DF2



## UDG

- $R_e > 1.5 \text{ kpc}$
- $\mu(g,0) > 24 \text{ mag arcsec}^{-2}$

## NGC1052–DF2

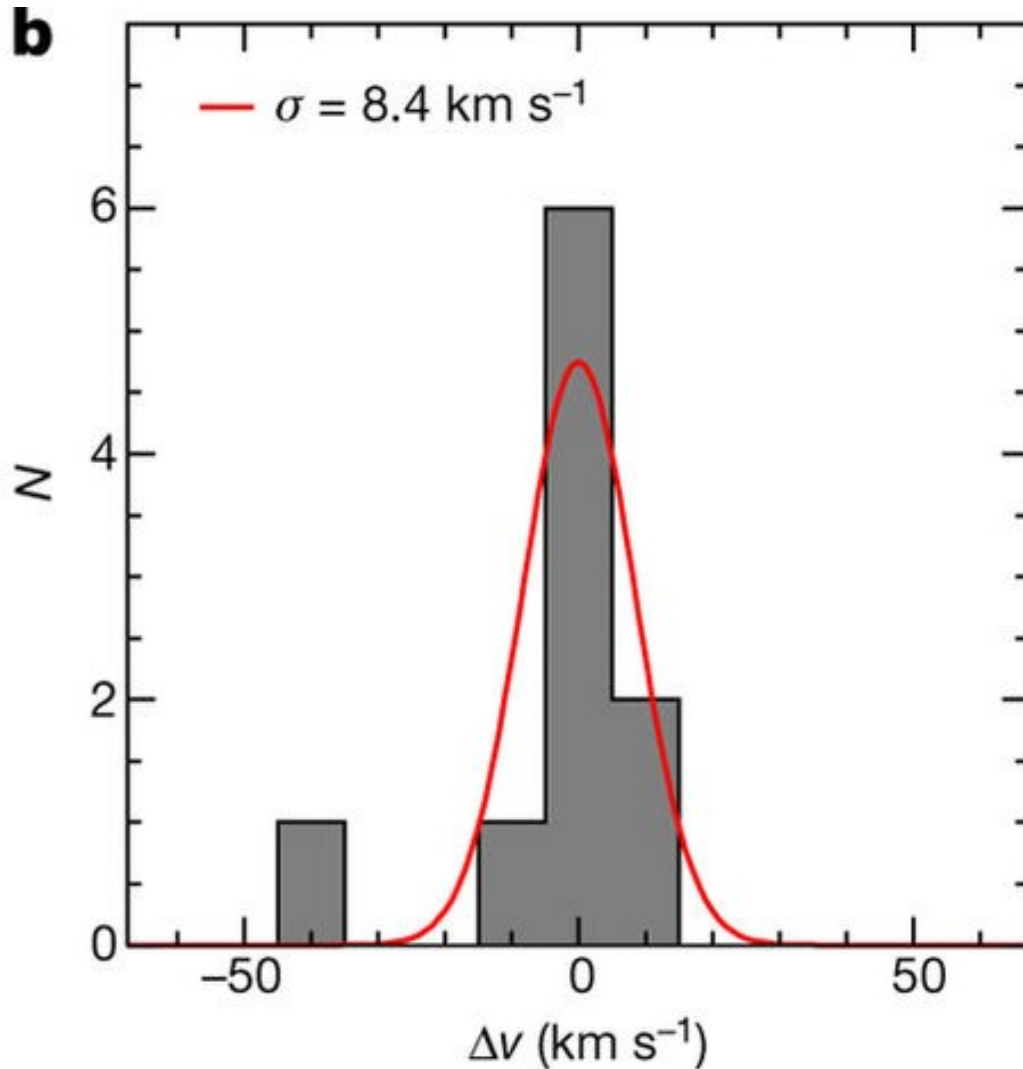
- $R_e = 2.2 \text{ kpc}$
- $\mu(g,0) = 24.4 \text{ mag arcsec}^{-2}$

Figure 1 | HST/Advanced Camera for Surveys (ACS) image of NGC1052–DF2. NGC1052–DF2 was identified as a large (approximately  $2'$ ) low-surface-brightness object, at right ascension  $\alpha = 2 \text{ h } 41 \text{ min } 46.8 \text{ s}$ , declination  $\delta = -8^\circ 24' 12''$  (J2000). HST imaging of NGC1052–DF2 was obtained on 2016 November 10, using the ACS. The exposure time was 2,180 s in the  $V_{606}$  filter and 2,320 s in the  $I_{814}$  filter. The image spans  $3.2' \times 3.2'$ , or  $18.6 \text{ kpc} \times 18.6 \text{ kpc}$  at the distance of NGC1052–DF2; north is up and east is to the left. Faint striping is caused by imperfect charge-transfer-efficiency removal. Ten spectroscopically confirmed luminous compact objects are marked.

**nature**



# Kinematics in NGC1052–DF2



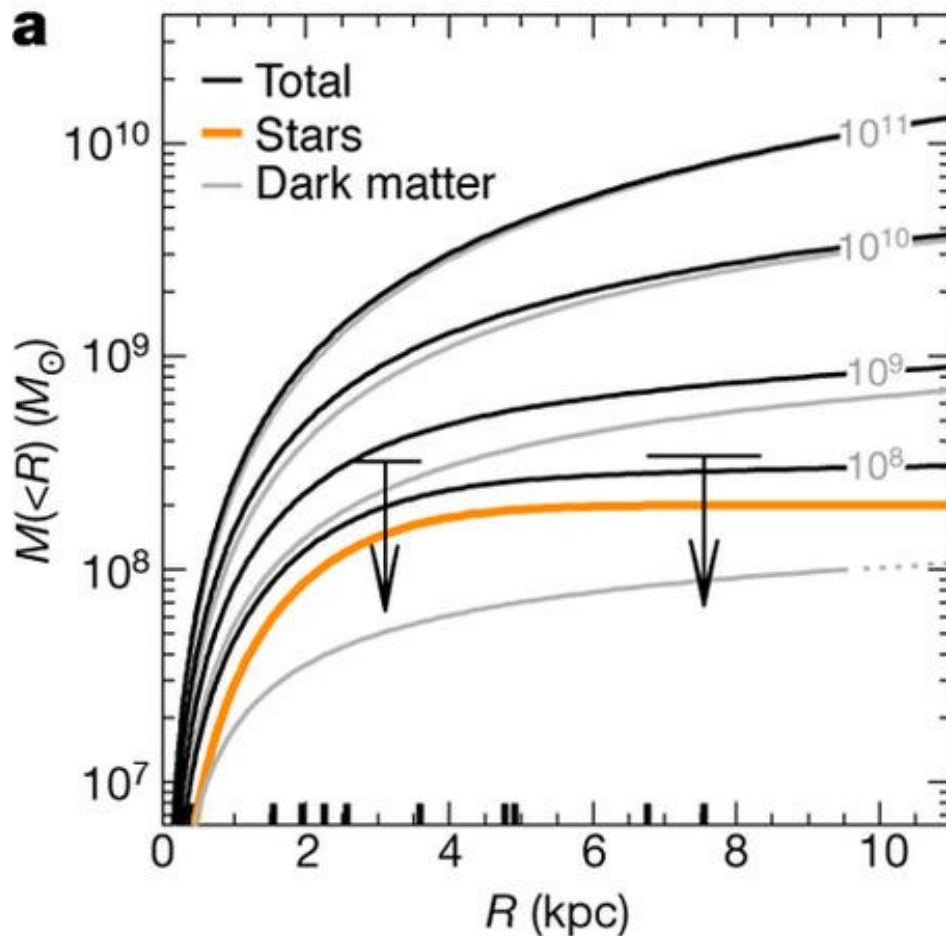
The 90% confidence upper limit

$$\sigma_{\text{intr}} < 10.5 \text{ km s}^{-1}$$

**Figure 3 | Velocity dispersion.** The filled grey histograms show the velocity distribution of the ten compact objects. **a**, Wide velocity range including the velocities of all 21 galaxies in the NASA/IPAC Extragalactic Database with  $cz < 2,500 \text{ km s}^{-1}$  that are within a projected distance of two degrees from NGC 1052. The red dotted curve shows a Gaussian with a width of  $\sigma = 32 \text{ km s}^{-1}$ , the average velocity dispersion of Local Group galaxies with  $8.0 \leq \log(M_{\text{stars}}/M_{\odot}) \leq 8.6$ . **b**, Narrow velocity range centred on  $cz = 1,803 \text{ km s}^{-1}$ . The red solid curve is a Gaussian with a width that is equal to the biweight dispersion of the velocity distribution of the compact objects,  $\sigma_{\text{obs}} = 8.4 \text{ km s}^{-1}$ . Taking observational errors into account, we derive an intrinsic dispersion of  $\sigma_{\text{intr}} = 3.2^{+5.5}_{-3.2} \text{ km s}^{-1}$ , with the uncertainties 1 s.d. The 90% confidence upper limit on the intrinsic dispersion is  $\sigma_{\text{intr}} < 10.5 \text{ km s}^{-1}$ .

# A galaxy lacking dark matter

Pieter van Dokkum<sup>1</sup>, Shany Danieli<sup>1</sup>, Yotam Cohen<sup>1</sup>, Allison Merritt<sup>1,2</sup>, Aaron J. Romanowsky<sup>3,4</sup>, Roberto Abraham<sup>5</sup>, Jean Brodie<sup>4</sup>, Charlie Conroy<sup>6</sup>, Deborah Lokhorst<sup>5</sup>, Lamiya Mowla<sup>1</sup>, Ewan O'Sullivan<sup>6</sup> & Jielai Zhang<sup>5</sup>



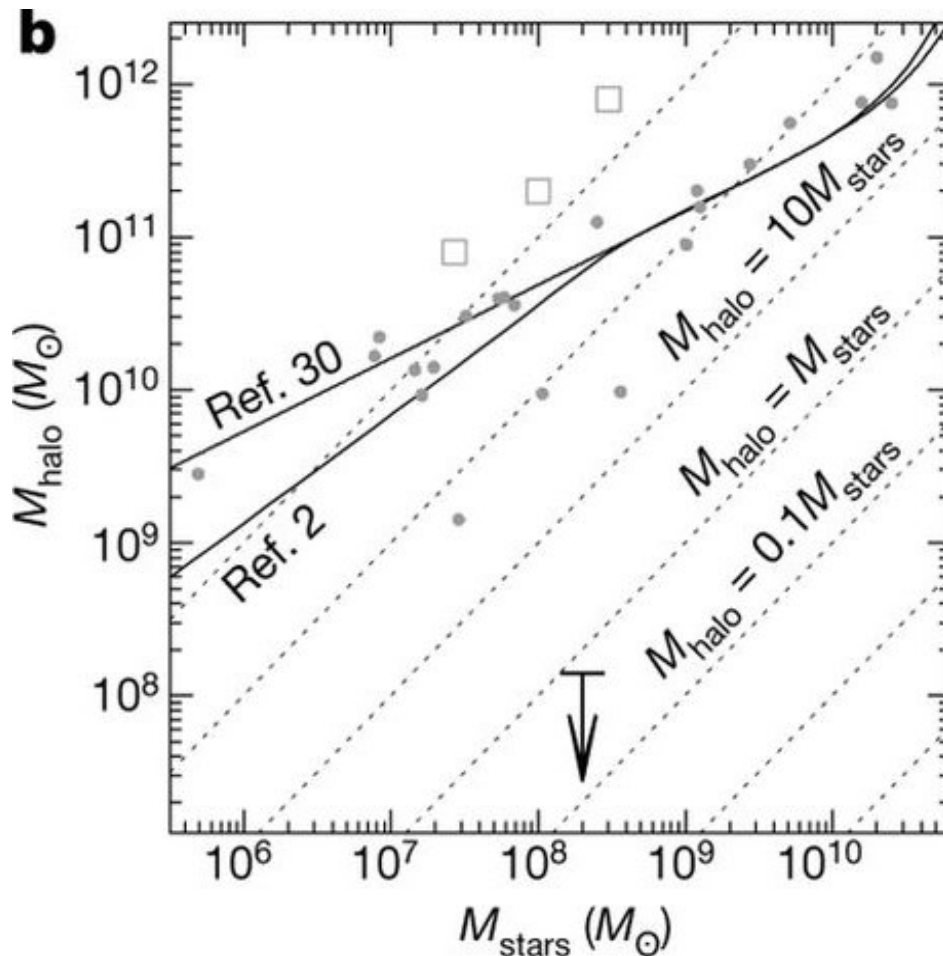
The **orange curve** is the stellar mass component.

$M_{\text{dyn}} < 3.2 \times 10^8 M_{\odot}$  within  $R_{\text{out}} = 3.1$  kpc

$M_{\text{dyn}} < 3.4 \times 10^8 M_{\odot}$  within  $R_{\text{out}} = 7.6$  kpc

## A galaxy lacking dark matter

Pieter van Dokkum<sup>1</sup>, Shany Danieli<sup>1</sup>, Yotam Cohen<sup>1</sup>, Allison Merritt<sup>1,2</sup>, Aaron J. Romanowsky<sup>3,4</sup>, Roberto Abraham<sup>5</sup>, Jean Brodie<sup>4</sup>, Charlie Conroy<sup>6</sup>, Deborah Lokhorst<sup>5</sup>, Lamiya Mowla<sup>1</sup>, Ewan O'Sullivan<sup>6</sup> & Jielai Zhang<sup>5</sup>



**Halo mass – stellar mass relation**

**NGC1052-DF2**

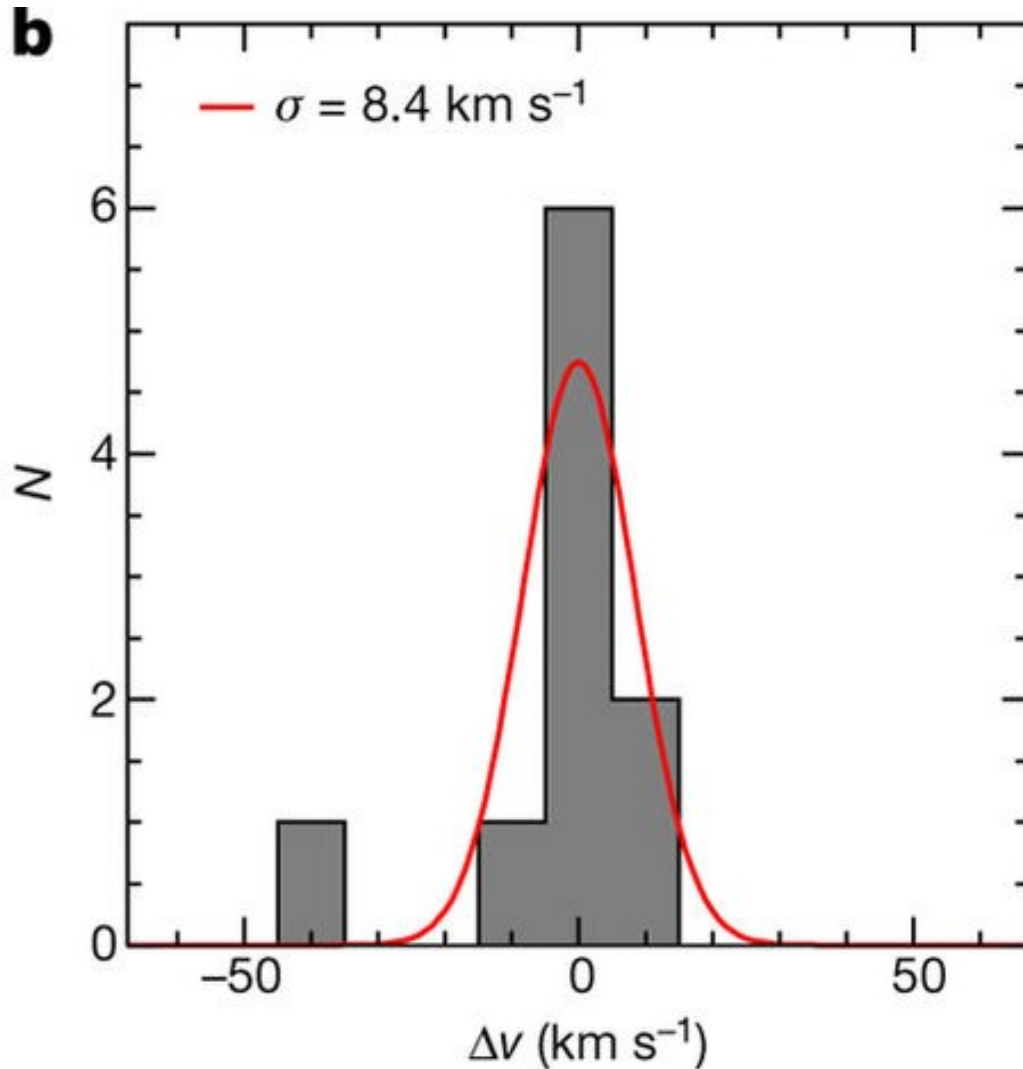
$$M_{\text{stars}} = 3.4 \times 10^8 M_{\odot}$$

**The expected  $M_{\text{halo}} \approx 6 \times 10^{10} M_{\odot}$**

**It is about 400 higher than the upper limit.**



# Disfavor in MOND?



**Velocity Dispersion in MOND  
without considering “external field  
effect”**

$$\sigma_M \approx (0.05 G M_{\text{stars}} a_0)^{1/4}$$

$$\approx 20 \text{ km s}^{-1}$$

**Figure 3 | Velocity dispersion.** The filled grey histograms show the velocity distribution of the ten compact objects. **a**, Wide velocity range including the velocities of all 21 galaxies in the NASA/IPAC Extragalactic Database with  $cz < 2,500 \text{ km s}^{-1}$  that are within a projected distance of two degrees from NGC 1052. The red dotted curve shows a Gaussian with a width of  $\sigma = 32 \text{ km s}^{-1}$ , the average velocity dispersion of Local Group galaxies with  $8.0 \leq \log(M_{\text{stars}}/M_{\odot}) \leq 8.6$ . **b**, Narrow velocity range centred on  $cz = 1,803 \text{ km s}^{-1}$ . The red solid curve is a Gaussian with a width that is equal to the biweight dispersion of the velocity distribution of the compact objects,  $\sigma_{\text{obs}} = 8.4 \text{ km s}^{-1}$ . Taking observational errors into account, we derive an intrinsic dispersion of  $\sigma_{\text{intr}} = 3.2^{+5.5}_{-3.2} \text{ km s}^{-1}$ , with the uncertainties 1 s.d. The 90% confidence upper limit on the intrinsic dispersion is  $\sigma_{\text{intr}} < 10.5 \text{ km s}^{-1}$ .

# CURRENT VELOCITY DATA ON DWARF GALAXY NGC1052-DF2 DO NOT CONSTRAIN IT TO LACK DARK MATTER

NICOLAS F. MARTIN<sup>1,2</sup>, MICHELLE L. M. COLLINS<sup>3</sup>, NICOLAS LONGEARD<sup>1</sup>, ERIK TOLLERUD<sup>4</sup>

*Draft version April 13, 2018*

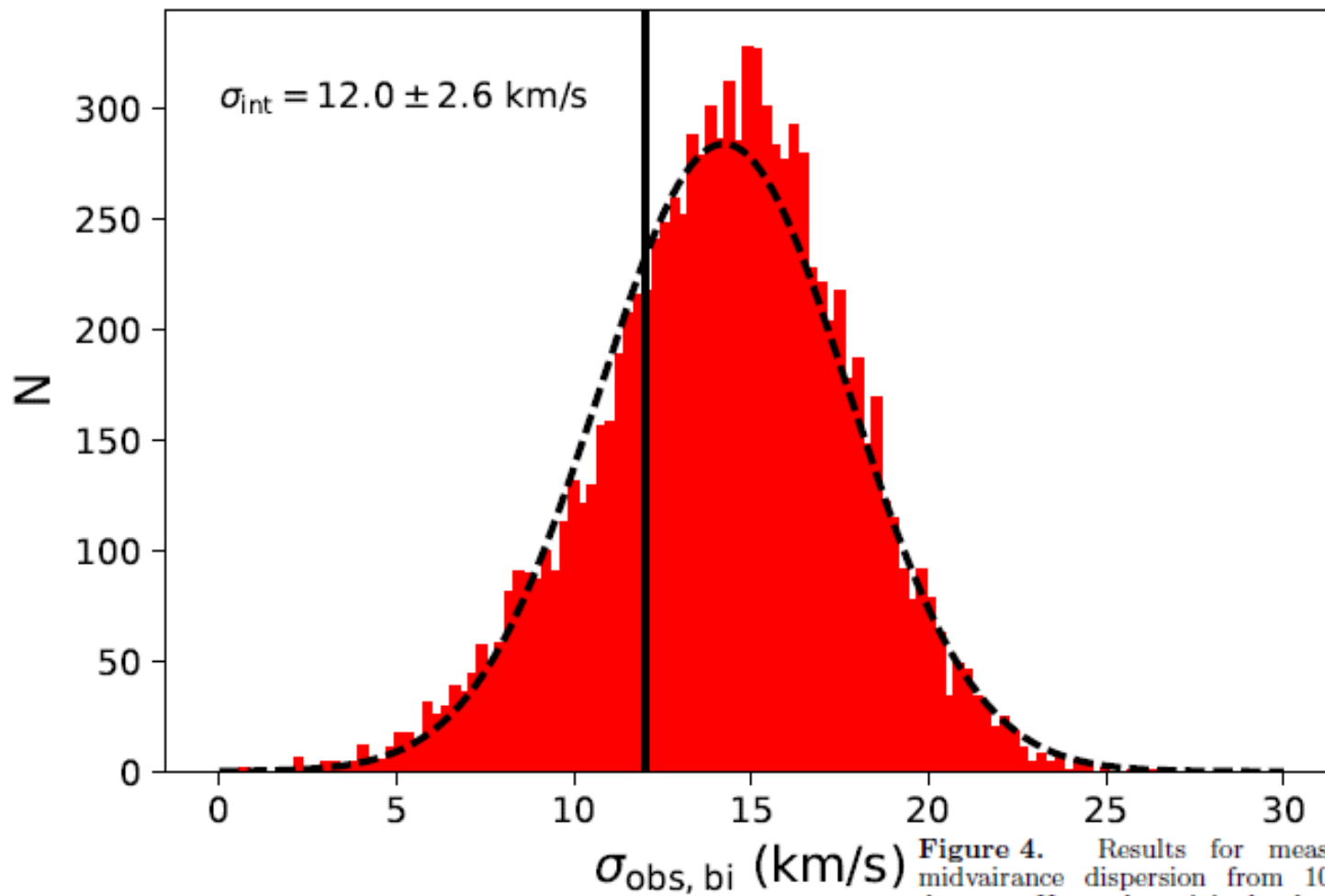
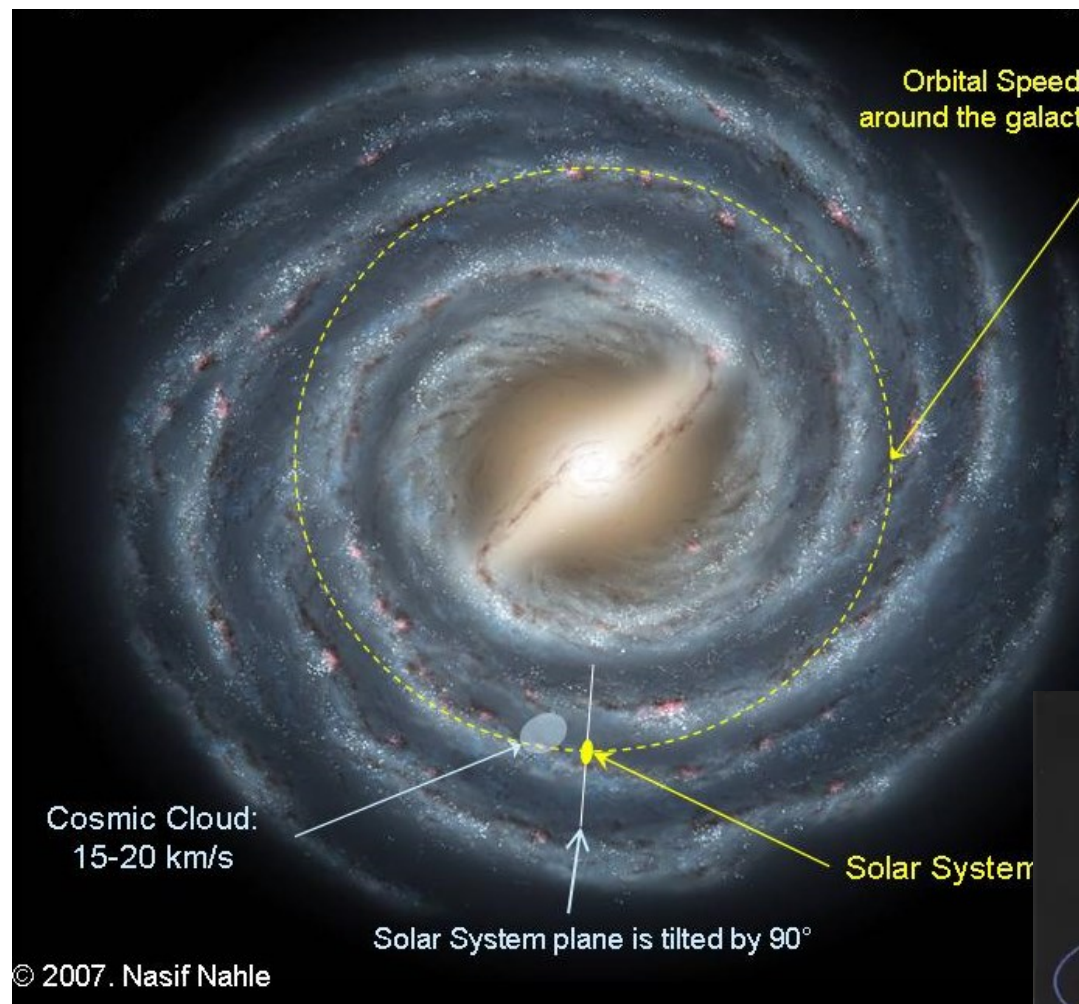


Figure 4. Results for measuring the observed biweight-midvariance dispersion from 10,000 resamples of the vD18b dataset. Here, the original velocities are perturbed within their  $1\sigma$  uncertainties as described in the text. The mean observed biweight for the sample comes out as  $\sigma_{\text{obs, bi}} = 14.3 \pm 3.5$  km s<sup>-1</sup>, giving  $\sigma_{\text{int, bi}} = 12.0 \pm 2.5$  km s<sup>-1</sup>, higher than the 90% upper limit from vD18b, and consistent with our MCMC analysis.

# External Field Effect in MOND

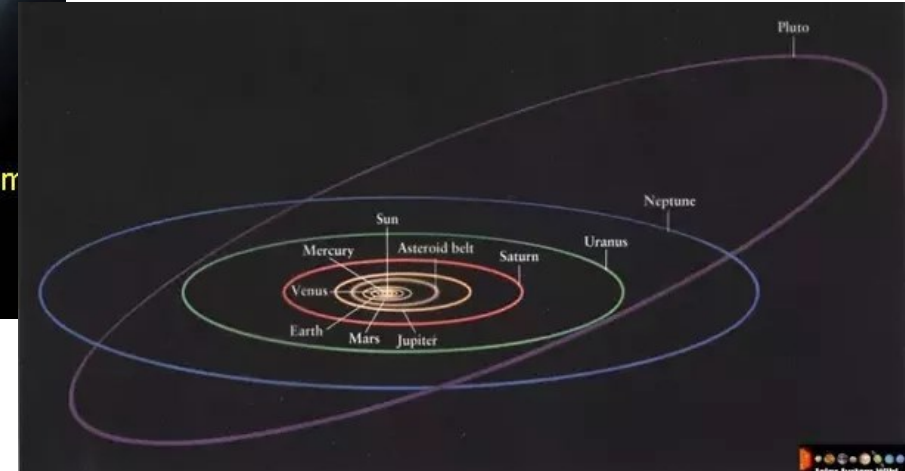


The Solar system is well described by Newtonian Dynamics.

The center of the solar system rotates the Milky Way in MOND regime  $10^{-10} \text{ ms}^{-2}$ .

Why?

$$\mu(g_0/a_0) \cdot g_0 = \nabla \cdot \varphi$$



# MOND and the dynamics of NGC1052-DF2

B. Famaey,<sup>1★</sup> S. McGaugh,<sup>2</sup> and M. Milgrom<sup>3</sup>

<sup>1</sup>*Université de Strasbourg, CNRS UMR 7550, Observatoire astronomique de Strasbourg, 67000 Strasbourg, France*

<sup>2</sup>*Department of Astronomy, Case Western Reserve University, Cleveland, OH 44106, USA*

<sup>3</sup>*Department of Particle Physics and Astrophysics, Weizmann Institute of Science, Rehovot 76100, Israel*

$$(g + g_e) \mu \left( \frac{g + g_e}{a_0} \right) = g_N + g_e \mu \left( \frac{g_e}{a_0} \right),$$

$$\sigma_{\text{MOND}} \approx 13.4 \text{ km s}^{-1}.$$

**For MOND,  $\sigma = 9.7\text{-}18.2 \text{ km s}^{-1}$**

$$\sigma_{\text{obs,bi}} = 14.3 \pm 3.5 \text{ km s}^{-1}$$

$$\sigma_{\text{int.bi}} = 12.0 \pm 2.5 \text{ km s}^{-1}$$



# Cluster Abell 520

- Abell 520 is a counter example of 1E 0657-558
- Weak lensing mass reconstruction matches with the central X-ray hot gas but leaves empty to galaxies.
- Member galaxies “X”
- Bright galaxies “orange” (Mahdavi et al. 2007)



Figure 1.7: The “cosmic train wreck” Cluster: Abell 520. Optical image of Abell 520 is from Canada-France-Hawaii Telescope. The hot gas is shown by Chandra X-ray image (red color). Weak lensing contour shows surface mass density (blue color). Member galaxies and bright galaxies are marked with a X and orange color respectively. (Mahdavi et al. (2007))

# Bullet Cluster 1E 0657-558

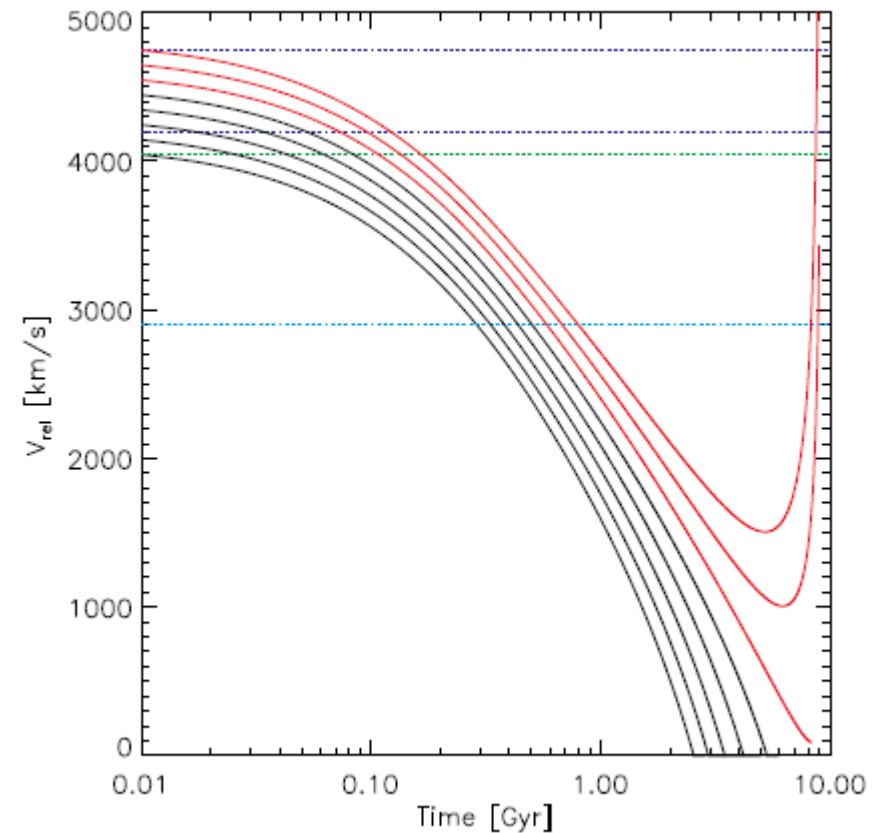
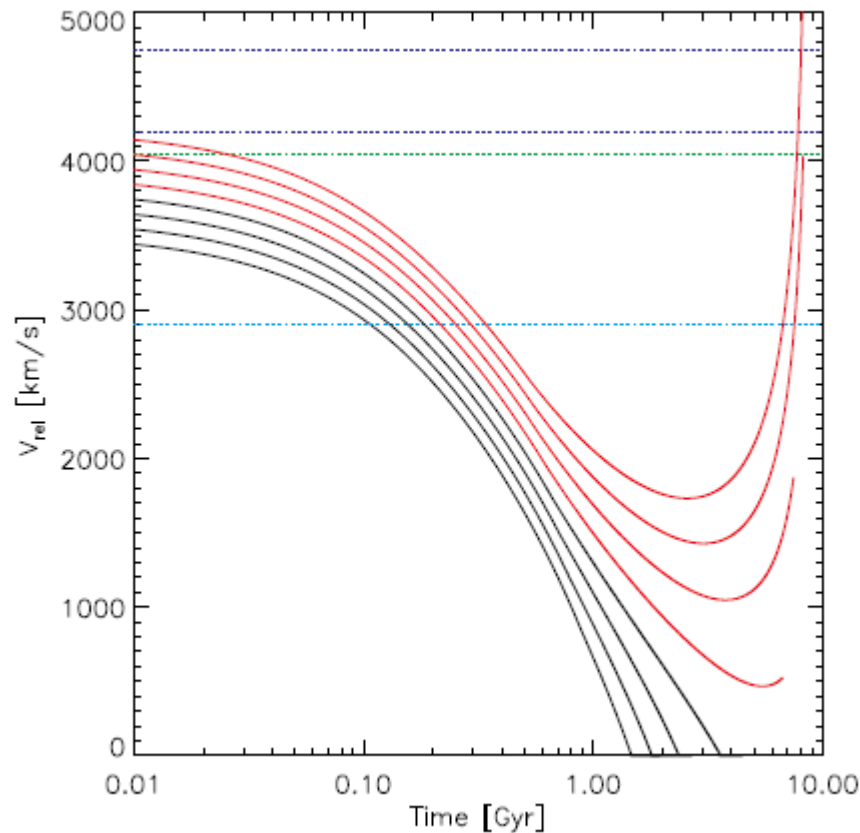


Figure 5.4: **Relative Velocity of Two Clusters in 1E0657-558.** Time=0Myr is the current ( $z=0.3$ ) relative velocity of the two clusters with larger times corresponding to higher redshifts. Black lines correspond to relative velocities that are achievable, whereas red lines are not. *Left Panel:* In CDM model simulation, The relative velocities used are  $v_{\text{rel}}=3500\text{--}4200\text{ km s}^{-1}$  in intervals of  $100\text{ km s}^{-1}$ . *Right Panel:* In MOND simulation with the standard form, The relative velocities used are  $v_{\text{rel}}=4100\text{--}4800\text{ km s}^{-1}$  in intervals of  $100\text{ km s}^{-1}$ . The high observed collision velocity is more readily obtained in MOND than CDM. (Angus & McGaugh (2008))



# External Field Effect in MOND

McGaugh (2007)

Newtonian regime

$$g_{in} > a_0 \quad M = \frac{RV^2}{G}$$



e.g.,  
surface  
of the  
Earth

MOND regime

$$g_{in} < a_0 \quad M = \frac{V^4}{a_0 G}$$



e.g.,  
remote  
dwarf  
Leo I

isolated systems

External Field dominant  
Newtonian regime

$$g_{in} < a_0 < g_{ex} \quad M = \frac{RV^2}{G}$$

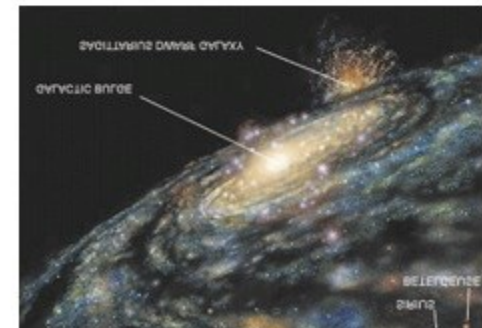


e.g.,  
Globular  
cluster  
M13

non-isolated systems

External Field dominant  
quasi-Newtonian regime

$$g_{in} < g_{ex} < a_0 \quad M = \frac{g_{ex}}{a_0} \frac{RV^2}{G}$$



e.g.,  
nearby  
Sgr  
dwarf